

# Quantum Private Distributed Matrix Multiplication With Degree Tables

Mohamed Nomeir   Alptug Aytekin   Lei Hu   Sennur Ulukus

Department of Electrical and Computer Engineering

University of Maryland, College Park, MD 20742

*mnomeir@umd.edu   aaytekin@umd.edu   leihu@umd.edu   ulukus@umd.edu*

## Abstract

In this paper, we explore how quantum resources can be used to increase the rate of private distributed matrix multiplication (PDMM). In PDMM, a user who has two high-dimensional matrices,  $A$  and  $B$ , and lacks the computational capabilities to apply matrix multiplication locally, divides the matrices  $A$  and  $B$  into  $K$  and  $L$  sub-blocks, respectively. Then, the user sends them to  $N$  servers to apply the required multiplication *privately*, i.e., any  $T$  colluding servers cannot get any information about the user's matrices. The goal is to reduce the number of servers needed to perform the required matrix multiplication, thereby decreasing the communication cost. In the quantum setting, we allow the servers to share an entangled state, amongst each other only, and respond back to the user over separate quantum channels. Upon receiving the quantum dits, the user should be able to obtain the required matrix multiplication by applying the appropriate measurements. There are two main regimes in the PDMM literature (assuming  $K \geq L$ , without loss of generality): The first regime is when the privacy parameter  $T$  is high compared to  $K$  or  $L$ , i.e.,  $T > K \geq L$  or  $K \geq T \geq L$ , called the high-privacy regime. In the second regime, the low-privacy regime, the privacy parameter  $T$  is less than  $K$  and  $L$ , i.e.,  $K \geq L > T$ .

First, in the high-privacy regime, the state-of-the-art classical code is called the gap additive secure polynomial (GASP) code. We define a feasibility requirement in the quantum setting for the GASP code such that the highest performance is achieved when the requirement is satisfied. Thus, super-dense coding gain is achieved when the feasibility condition is satisfied. In the case when the feasibility condition is not satisfied, we address two main concerns. The first is to find a relation between the minimum privacy requirement and the dimensions of the two matrices needed for the feasibility condition to be satisfied, i.e., we quantify the limitation for satisfying the aforementioned feasibility requirement. We provide a second-degree polynomial estimate for the aforementioned relation. Second, we develop a new family of codes that can work in the quantum setting, and show that it outperforms the classical GASP

code with different gains based on the regime and specific values of  $K$  and  $L$ . Notably, the super-dense coding gain can still be achieved by the new codes in certain cases compared to the corresponding classical GASP codes with the same parameters.

Second, since GASP does not work efficiently in the low-privacy regimes compared to two codes that were recently developed, namely cyclic-addition degree tables (CAT) and discretely optimized GASP (DOG), we show that the feasibility condition developed for GASP can be adopted for both CAT and DOG codes as well, thus unifying the feasibility framework for multiple classical PDMM coding schemes. In addition, we propose another set of codes that can be used in the low privacy regime in the quantum setting when the feasibility requirement is not satisfied. We compare its rate with its classical counterpart. The techniques we adopt for this new family of codes in the low privacy regimes are inspired by the quantum private information retrieval (QPIR) setting when the privacy requirement is low.

## 1 Introduction

Matrix multiplication (MM) is a key component in all machine learning (ML), artificial intelligence (AI), and signal processing (SP) tasks [1–3]. Due to the high dimensionality of the data, matrix multiplication often involves high-dimensional matrices that cannot be computed or processed using a single personal computer. The idea of relaying these operations to more computationally capable entities, which we call servers, was introduced to address this limitation in the computer science community [4–9]. The user who distributes the matrices to the servers seeks to preserve the privacy of the data. Thus, the main goal is to hide as much information about these matrices as possible from the computing servers, while ensuring low computation complexity and high download rates. Recently, the problem has been adopted into the communications and information theory communities, and it was first formalized by [10]. In [10], the problem was formulated as a user who has two matrices,  $A$  and  $B$ , for which the user does not have the capabilities to compute their product. The user sends a coded version of each matrix to ensure privacy, after slicing  $A$  horizontally and  $B$  vertically, to  $N$  servers to compute the multiplication of the coded versions and transmit the multiplication back to the user.

There are two privacy settings adopted in [10]. The first requires that the two matrices,  $A$  and  $B$ , to be kept *information-theoretically* private from any  $T$  curious but honest servers that share their coded versions with each other. The main performance metric is the download rate, i.e., the number of useful multiplications over the number of downloaded symbols. The second setting in [10] analyzes the case when  $A$  is kept private but  $B$  is public knowledge. The latter setting is not considered in this paper, and we only consider the first case with  $A$  and  $B$  being private. The approach for slicing  $A$  horizontally into  $K$  sub-matrices and  $B$  vertically into  $L$  sub-matrices and transmitting them to the curious servers appears to increase the total computational requirements compared to the single computer at the user

side due to the privacy requirement. This concern was echoed in [11]. However, in [12], it was shown that indeed *this is not the case*, and computational complexity can be optimized if the correct partitioning is used. Finally, the act of slicing  $A$  horizontally and  $B$  vertically and requiring  $AB$  computed is called outer product partitioning (OPP), and it is the main focus in this paper. If the required product is  $BA$ , then it is called inner product partitioning (IPP); see e.g., [13–15]. Other works have considered more general frameworks for both the IPP and OPP, e.g., in [16–21].

Since the OPP problem is a critical step in a wide range of applications such as GPU acceleration, tensor contractions and deep learning [22–24], many works have studied the OPP problem defined in [10] in different contexts. In [25, 26], bivariate and multivariate polynomials are used to encode the submatrices. Specifically, bivariate polynomials are sufficient to be used in the case of homogeneous upload cost thresholds, and multivariate polynomials are suitable for the case of stragglers. In [27], the case where the user has some information about the multiplication of the noise matrices is analyzed. In [28], the OPP problem is studied in the context of algebraic geometric codes. In [29], successive cancellation is used to obtain an approximate result for the computation of  $AB$  that becomes more accurate with time.

A widely adopted technique for OPP is called gap additive secure polynomial (GASP) method, developed in [30]. GASP utilizes polynomial codes and selects polynomials to minimize the required number of servers. Until recently, GASP was regarded as the state-of-the-art for the PDMM OPP across all privacy regimes. However, in a recent work, [31] introduced three novel code constructions. The three codes are modified versions of GASP: 1) optimized GASP, which provides better rates than GASP in general at the expense of requiring high computational power to find the optimal number of servers, 2) the cyclic-addition degree tables (CAT), and 3) the discretely optimized GASP (DOG). Both CAT and DOG outperform GASP or optimized GASP in low-privacy regimes, while optimized GASP consistently outperforms GASP. The first reason we adopt GASP over optimized GASP is the computational complexity, especially when the sub-packetization of the matrices and the privacy requirement are high, i.e., when  $K$ ,  $L$  and  $T$  are large, since the optimal value of the number of servers is found by trial and error over two free parameters (related to  $K$  and  $T$ ) as opposed to one free parameter for GASP. The second reason we adopt GASP over optimized GASP is that the normal GASP is more likely to satisfy the required feasibility constraint we developed to extend to the quantum version, compared to the optimized GASP, according to our trials. When the feasibility requirement is satisfied, the classical code can be extended to the quantum code, achieving double-the-rate of its classical counterpart.

Concurrently, quantum communications has gained significant attention recently due to its potential in increasing the fundamental limits of communication compared to classical communications. It was shown in [32] that pre-entanglement between the transmitter and the receiver can double the communication rate, i.e., a single qubit can carry two bits of

useful information, which was coined as *super-dense coding*. The setting where  $N$  entangled transmitters communicate over a noiseless quantum channel to a receiver was re-formalized in [33]. In that setting, at most  $N$  useful bits can be received by the receiver. In classical communication with no other requirement, this restriction implies that no gain can be achieved in using the quantum resources compared to the classical ones. However, this setting showed great promise in both the quantum private information retrieval (QPIR) setting and the quantum computation setting, where super-dense coding gain was achieved, as shown in [34–42]. The setting in [33] and the corresponding formulation, using specific encoding and decoding, was coined as the  *$N$ -sum box abstraction*.

In this paper, we aim to develop a framework for PDMM that extends the classical codes and provide new quantum PDMM codes in the setting where the transmitters are entangled. We aim to improve the communication efficiency of PDMM in the multiple to one quantum network. The main contributions of our work are summarized as follows:

- We formulate the PDMM problem in the quantum communication framework and study the problem in two different regimes, the low privacy regime and the high privacy regime, respectively.
- For the high privacy regime, we consider the GASP codes and study how they can be extended to the quantum setting. We provide a feasibility condition, such that, when satisfied, classical GASP can be extended to the quantum setting, maintaining the same number of servers while doubling the download rate compared to its classical counterpart, i.e., achieving super-dense coding gain.
- The feasibility condition we develop is not always satisfied by the GASP code for all  $K$ ,  $L$  and  $T$ . Thus, we provide an approximate estimate for the minimum  $T$  needed for the feasibility condition to be satisfied. The estimated relation is a second-degree polynomial for  $K$  and  $L$ .
- We develop a new family of polynomial codes that are designed solely for the quantum setting for the high privacy regime to mitigate the aforementioned issue and achieve better rates compared to the classical setting.
- For the low privacy regime, we utilize the aforementioned three codes in [31], and show that the feasibility condition defined for GASP can be utilized for them as well, thus unifying the approach. Specifically, we focus on CAT and DOG codes since they provide higher rates compared to the GASP codes and the optimized GASP codes in low privacy regimes. We provide an explicit example where the CAT code surpasses all the aforementioned codes and satisfies the feasibility constraint, and thus, we achieve double-the-rate compared to the highest possible classical rate to date.
- In addition, inspired by the QPIR problem, we provide a technique to design quantum PDMM polynomial codes when the feasibility requirement is not satisfied. Our main

idea here stems from increasing the privacy constraint  $T$ , to provide higher than the classical setting, however, not achieving super-dense coding gain.

We summarize our results and findings as follows. We extend the GASP codes to their quantum counterpart via a feasibility condition that we developed. When the condition is satisfied, we can apply our proposed scheme to double the download rate. Also, we show that the feasibility condition is always satisfied when  $T \sim KL$ . Furthermore, we focus on the classical codes that are efficient in the low privacy regime. We extend the modified GASP, CAT, and DOG codes using the same feasibility condition, thus unifying the framework. We note that, when the privacy requirement is low, it is hard to find a case when CAT and DOG surpass the GASP code and satisfy the feasibility condition at the same time. However, we show that when  $K = L = T = 2$ , the CAT code surpasses all the classical PDMM OPP codes and satisfies the feasibility requirement. In the case where the feasibility condition is not satisfied in the high privacy regime, we develop a separate set of codes that work directly in the quantum setting. We compare the developed codes and their classical counterparts in terms of the download rate. The results show that the rate for these quantum codes varies from double the classical rate to identical rate depending on the relation between  $T$ ,  $L$  and  $K$ . In addition, for the low privacy setting, we develop quantum codes, inspired by the previous work in the QPIR literature. We compare these quantum codes with their classical counterparts in terms of download cost. The results show that the highest gain is 1.5 due to the low privacy requirement.

The paper is organized as follows. Section 2 reviews important topics related to our work, namely, generalized Reed-Solomon (GRS) and dual GRS codes, quantum information theory, and the  $N$ -sum box abstraction. In addition, we provide some important minor extension results that are needed in our paper. Section 3 formulates the PDMM problem in the classical and quantum settings. Section 4 focuses on GASP codes for the high privacy regime. In Section 4, we review the classical GASP code, then we provide a condition such that, if satisfied, the GASP code can be extended to the quantum version and achieve super-dense coding gain. In Section 5, we develop a family of quantum PDMM codes that do not require the same condition as the GASP code; in addition, we compare the rate of these codes with the classical GASP over a range of varying parameters. In Section 6, we review the classical PDMM codes that achieve better rates compared to the GASP code in the low privacy regime and use the same condition to extend them to the quantum version. In addition, we provide a detailed example in this case to show that the super-dense coding gain can be achieved if the aforementioned condition is satisfied. Finally, in Section 7, we develop a family of codes that works in the low privacy regime when the feasibility requirement is not satisfied and compare it with the aforementioned classical codes.

**Notation:** Prior to delving into the next sections, we explicitly mention the general notations we use, except stated otherwise, for the paper. We denote the natural numbers as

$\mathbb{N} = \{0, 1, 2, \dots\}$ . Let  $\alpha \in \mathbb{N}^{K+T}$  and  $\beta \in \mathbb{N}^{L+T}$ , then we denote

$$\alpha \oplus \beta = \begin{bmatrix} \alpha_1 + \beta_1 & \alpha_1 + \beta_2 & \dots & \alpha_1 + \beta_{L+T} \\ \alpha_2 + \beta_1 & \alpha_2 + \beta_2 & \dots & \alpha_2 + \beta_{L+T} \\ \vdots & \vdots & \ddots & \vdots \\ \alpha_{K+T} + \beta_1 & \alpha_{K+T} + \beta_2 & \dots & \alpha_{K+T} + \beta_{L+T} \end{bmatrix}. \quad (1)$$

If  $A \in \mathbb{R}^{m \times n}$ , then let  $\text{Set}(A)$  denote the set with the elements of the matrix  $A$ . We use the superscript  $t$  for the transpose operator, with computational basis as the main basis, and  $\dagger$  is the conjugate transpose operator.  $[n]$  denotes the set  $\{1, \dots, n\}$ , and  $[a : b]$  denotes the set  $\{a, a+1, \dots, b\}$ . For a matrix  $A \in \mathbb{R}^{m \times n}$ ,  $A(:, [a : b])$  defines a sub-block of the aforementioned matrix with all the rows included and the columns chosen are those indexed by the set  $[a : b]$ . All vectors are column vectors except stated otherwise. All symbols that denote sets are written using a calligraphic font. If  $\mathcal{S}$  is a set, then  $\mathcal{S}(m)$  denotes the  $m$ th element in the set after a predefined indexing. If  $a$  is any constant, then  $a^{\mathcal{S}} = [a^{\mathcal{S}(1)}, \dots, a^{\mathcal{S}(|\mathcal{S}|)}]$ . If  $K$  is a constant and  $a = [a_1, \dots, a_n]$ , then,  $K + a = K\mathbf{1}^t + a$ , where  $\mathbf{1}$  is the all ones vector with the required length. We use  $\mathbb{1}_{\mathcal{S}}$  is an indicator random variable for the occurrence of the event  $\mathcal{S}$ .  $I_N$  is the identity matrix of size  $N$ . Uppercase letters are used for matrices, and lowercase letters are used for vectors. Constants are written in upper or lower case fonts depending on the situation, and will be mentioned if not clear from the context. Finally, for the quantum systems and quantum operators, we use upper case with typewriter font, and for the associated quantum density matrix, as a special case of quantum operators, the Greek symbols  $\sigma$  and  $\rho$  are used.

## 2 Preliminaries

### 2.1 Dual Codes

Let  $C$  be a linear code in  $\mathbb{F}_q^n$ , the dual linear code of  $C$ ,  $C^\perp$ , is defined as

$$C^\perp = \{x \in \mathbb{F}_q^n : x^t c = 0, c \in C\}. \quad (2)$$

Since both are linear codes, they can be generated using generator matrices,  $G_C \in \mathbb{F}_q^{k \times n}$ , and  $G_{C^\perp} \in \mathbb{F}_q^{n-k \times n}$ , respectively. Then, both are connected with the following relation

$$G_C G_{C^\perp}^t = 0. \quad (3)$$

An important code family in this work is the GRS code and its dual [43]. The  $[n, k, d]_q$  GRS code is defined as follows.

**Definition 1 (GRS code)** Let  $F = \mathbb{F}_q$  be a field and choose  $n$  distinct non-zero elements

$\alpha_1, \dots, \alpha_n$ . Let  $u_1, \dots, u_n$  be non-zero elements in the field. Then, for any  $0 \leq k \leq n$ , the GRS is defined as

$$GRS(\alpha, u) = \{(u_1 f(\alpha_1), u_2 f(\alpha_2), \dots, u_n f(\alpha_n)) : f(x) \in F[x]_k\}, \quad (4)$$

where  $\alpha = \alpha_{[n]}$ ,  $u = u_{[n]}$ , and  $F[x]_k$  is the polynomial ring with degree less than  $k$ . In addition, the corresponding canonical generator matrix (transposed) is given by

$$G_{GRS(\alpha, u)} = \begin{bmatrix} u_1 & u_1 \alpha_1 & u_1 \alpha_1^2 & \dots & u_1 \alpha_1^{k-1} \\ u_2 & u_2 \alpha_2 & u_2 \alpha_2^2 & \dots & u_2 \alpha_2^{k-1} \\ \vdots & \vdots & \vdots & \ddots & \vdots \\ u_n & u_n \alpha_n & u_n \alpha_n^2 & \dots & u_n \alpha_n^{k-1} \end{bmatrix}. \quad (5)$$

For notational convenience, we henceforth refer to the transposed generator matrix simply as the generator matrix without loss of generality.

**Theorem 1 (Dual GRS)** *Given an  $[n, k, d_1]_q$  GRS code parameters with  $\alpha$  and  $u$  as the generating elements, the dual code is also a  $[n, n - k, d_2]_q$  GRS code with  $\alpha$  and  $v = v_{[n]}$  as the generating elements, where*

$$v_i = \frac{1}{u_i} \left( \prod_{\substack{j \in [n] \\ j \neq i}} (\alpha_j - \alpha_i) \right)^{-1}. \quad (6)$$

From Theorem 1, the generator matrix for the dual GRS can be written as

$$G_{GRS(\alpha, v)} = \begin{bmatrix} v_1 & v_1 \alpha_1 & v_1 \alpha_1^2 & \dots & v_1 \alpha_1^{n-k-1} \\ v_2 & v_2 \alpha_2 & v_2 \alpha_2^2 & \dots & v_2 \alpha_2^{n-k-1} \\ \vdots & \vdots & \vdots & \ddots & \vdots \\ v_n & v_n \alpha_n & v_n \alpha_n^2 & \dots & v_n \alpha_n^{n-k-1} \end{bmatrix}. \quad (7)$$

## 2.2 Dual of the Shifted GRS Code

**Definition 2 (Shifted GRS)** *An  $[n, k, d]_q$  GRS code is called  $\ell$ -shifted GRS if the generator matrix is defined as*

$$G_{GRS(\alpha, u)} = \begin{bmatrix} u_1 \alpha_1^\ell & u_1 \alpha_1^{\ell+1} & u_1 \alpha_1^{\ell+2} & \dots & u_1 \alpha_1^{\ell+k-1} \\ u_2 \alpha_2^\ell & u_2 \alpha_2^{\ell+1} & u_2 \alpha_2^{\ell+2} & \dots & u_2 \alpha_2^{\ell+k-1} \\ \vdots & \vdots & \vdots & \ddots & \vdots \\ u_n \alpha_n^\ell & u_n \alpha_n^{\ell+1} & u_n \alpha_n^{\ell+2} & \dots & u_n \alpha_n^{\ell+k-1} \end{bmatrix}. \quad (8)$$

**Theorem 2** *For any  $[n, k, d_1]_q$   $\ell_1$ -shifted GRS code with  $u$  and  $\alpha$  as the generating elements,*

there exists an  $[n, n - k, d_2]_q$   $\ell_2$ -shifted GRS code with  $v$  and  $\alpha$  as its dual code if

$$v_i = \frac{1}{u_i \alpha_i^{\ell_1 + \ell_2}} \left( \prod_{\substack{j \in [n] \\ j \neq i}} (\alpha_j - \alpha_i) \right)^{-1}. \quad (9)$$

This result follows directly by substituting (6) and plugging  $u_i$  as  $u_i \alpha_i^{\ell_1}$  and  $v_i$  as  $v_i \alpha_i^{\ell_2}$ , respectively.

## 2.3 Quantum Information Theory

For completeness, we recall the following standard definitions from quantum information theory. Detailed explanation and properties can be found in standard references on quantum information processing, e.g., [44].

**Definition 3 (Quantum density matrices)** *For a quantum system  $A$  that can be in the state  $|\psi_j\rangle$  with probability  $p_j$ , the quantum density matrix  $\rho_A$  is defined as*

$$\rho_A = \sum_j p_j |\psi_j\rangle \langle \psi_j|, \quad (10)$$

with  $p_j \geq 0$  and  $\sum_j p_j = 1$ .

**Definition 4 (Quantum operation)** *A quantum operation  $\mathbf{E}$  from the quantum system  $A$  to the quantum system  $B$  is a linear, completely-positive, and trace-preserving map from the set of all density operators of the Hilbert space representing  $A$  to the density operators of the Hilbert space representing  $B$ .*

**Definition 5 (Trace and partial trace)** *Given a quantum operator  $\mathbf{X}$  in a Hilbert space with dimension  $d$ , the trace operator is defined as*

$$\text{tr}(\mathbf{X}) = \sum_{i=0}^{d-1} \langle i | \mathbf{X} | i \rangle. \quad (11)$$

*In addition, given a composite quantum state  $\rho_{AB}$ , the partial trace for the quantum system  $A$  is given by*

$$\rho_B = \text{tr}_A(\rho_{AB}) = \sum_{i=0}^{d_A-1} (\langle i | \otimes I_{d_B}) \rho_{AB} (|i\rangle \otimes I_{d_B}), \quad (12)$$

where  $d_A$  and  $d_B$  are the dimensions of the Hilbert spaces associated with the quantum systems  $A$  and  $B$ , respectively.



**Theorem 3 (Kraus representation)** *Any quantum operation  $\mathbf{E}$  acting on a quantum state  $\rho$  can be written in the form*

$$\mathbf{E}(\rho) = \sum_i M_i \rho M_i^\dagger, \quad (13)$$

where  $\sum_i M_i^\dagger M_i = I$ .

## 2.4 $N$ -Sum Box Abstraction

The  $N$ -sum box abstraction describes an approach for encoding the classical dits onto quantum states when the transmitters are entangled [33]. The encoding and decoding structure in the  $N$ -sum box abstraction is described as follows. In the encoding stage, the servers use generalized Pauli operators  $\mathbf{X}(a) = \sum_{j=0}^{q-1} |j+a\rangle \langle j|$ , and  $\mathbf{Z}(a) = \sum_{j=0}^{q-1} \omega^{tr(aj)} |j\rangle \langle j|$ , where  $q = p^r$  with  $p$  being a prime number,  $a \in \mathbb{F}_q$  and  $\omega = \exp(2\pi i/p)$ , then transmit the resulting quantum states to the user over noise-free quantum channels.

In the decoding stage, the user applies a projection-valued measurement (PVM) defined on the quotient space of the stabilizer group  $\mathcal{L}(\mathcal{V})$  defined by

$$\mathcal{L}(\mathcal{V}) = \{c_v \mathbf{W}(v) : v \in \mathcal{V}\}, \quad (14)$$

where  $\mathcal{V}$  is a self-orthogonal subspace, with respect to the symplectic inner product in  $\mathbb{F}_q^{2N}$

$$\mathbf{W}(v) = \mathbf{X}(v_1) \mathbf{Z}(v_{N+1}) \otimes \dots \otimes \mathbf{X}(v_N) \mathbf{Z}(v_{2N}), \quad (15)$$

and  $c_v \in \mathbb{C}$  is chosen such that  $\mathcal{L}(\mathcal{V})$  is an Abelian subgroup of  $HW_q^N$  with  $c_v I_{q^N}$  being an element of the stabilizer group only with  $c_v = 1$ , where  $HW_q^N$  is the Heisenberg-Weyl group defined as follows

$$HW_q^N = \{c \mathbf{W}(s) : s \in \mathbb{F}_q^{2N}, c \in \mathbb{C} \setminus \{0\}\}. \quad (16)$$

**Theorem 4 (Theorem 1 in [33])** *Let  $G$  be a  $2N \times N$  SSO matrix, i.e.,  $G^t J G = 0$ , where  $J = \begin{bmatrix} 0 & I_N \\ -I_N & 0 \end{bmatrix}$ , and let  $H$  be a  $2N \times N$  matrix with full column rank. If  $[G \ H]$  is a full-rank matrix, then  $M = [0_N \ I_N][G \ H]^{-1}$  is a feasible  $N$ -sum box transfer matrix.*

A pictorial representation of the quantum circuit and its corresponding abstraction are given in Fig. 1 and Fig. 2. On the left side of Fig. 1, the two transmitters are entangled using the pure state  $|\beta_{00}\rangle = \frac{1}{\sqrt{2}}(|00\rangle + |11\rangle)$ , in addition, the receiver applies the Bell measurement on the two received qubits. On the right side of the same figure, an abstract matrix  $\mathbf{M}_{2 \times 4}$  is used to represent the relationship between the transmitted symbols  $a_1, a_2, b_1$ , and  $b_2$  with the received symbols after the Bell measurements, i.e.,  $a_1 + a_2$  and  $b_1 + b_2$ . Similarly, the left side

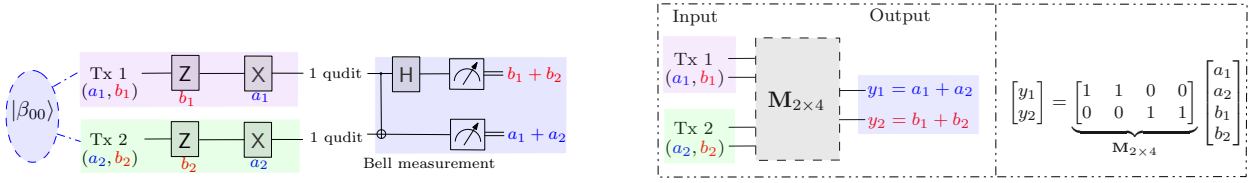


Figure 1: Quantum circuit for two entangled transmitters with the entangled state  $|\beta_{00}\rangle = \frac{1}{\sqrt{2}}(|00\rangle + |11\rangle)$  and the Bell measurement circuit on the left, and its 2-sum box abstraction on the right using the transfer matrix  $M_{2 \times 4}$  to represent the input-output relationship, i.e., the entangled state and the Bell measurement, for the circuit on the left.

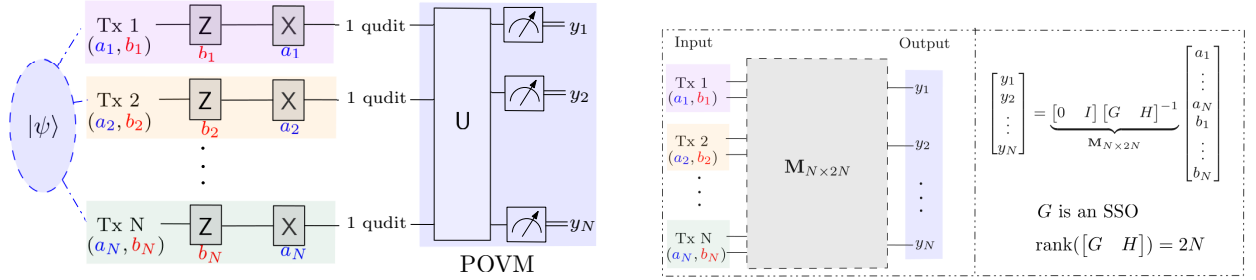


Figure 2: The general setting: Quantum circuit for  $N$  entangled transmitters with the entangled state  $|\psi\rangle$  with the corresponding quantum measurement circuit at the receiver side on the left, and its  $N$ -sum box abstraction on the right, using the transfer matrix  $M_{N \times 2N}$  to represent the input-output relationship, i.e., the entangled state and the measurement, for the circuit on the left.

of Fig. 2 represents a generalization for the 2-sum circuit with an arbitrary number of servers  $N$  sharing an entangled state  $|\psi\rangle$  and the receiver applying a general POVM measurement on the received  $N$  qudits. On the right side, the relation between the inputs from all the  $N$  transmitters  $(a_1, \dots, a_N, b_1, \dots, b_N)$ , where the  $i$ th transmitter sends  $(a_i, b_i)$ , and the  $N$  received symbols after measurement on the receiver side using the transfer matrix  $M_{N \times 2N}$ . The choice of a specific state  $|\psi\rangle$  and POVM measurements corresponds to a specific transfer matrix  $M_{N \times 2N}$ . Conversely, the choice of a specific value of  $M_{N \times 2N}$  satisfying the required conditions in Theorem 4 corresponds to one particular choice of  $|\psi\rangle$  and POVM.

### 3 Problem Formulation

We now formulate the PDMM problem in the classical and quantum setting, respectively.

In the classical setting, a user possessing two matrices  $A$  and  $B$ , with constrained local computational resources, seeks to compute their product. These matrices are divided into

$K$  and  $L$  sub-blocks, respectively, as follows

$$A = \begin{bmatrix} A_1 \\ A_2 \\ \vdots \\ A_K \end{bmatrix}, \quad B = [B_1, B_2, \dots, B_L], \quad (17)$$

where all  $A_i B_j$  are compatible for computing the outer product, i.e.,  $AB$ . Given  $K$  and  $L$ , the user distributes the encoded versions of the matrices to  $N$  servers, such that, these matrices are secure against any  $T$  colluding servers, i.e.,

$$I(f_{\mathcal{T}_1}, g_{\mathcal{T}_2}; A, B) = 0, \quad (18)$$

where  $f_i$  and  $g_i$  are the information sent by the user to the  $i$ th server about  $A$  and  $B$ , respectively.<sup>1</sup> In addition,  $\mathcal{T}_i \subset [N]$ , with  $|\mathcal{T}_i| \leq T$ ,  $i \in [2]$ .

**Remark 1** *Throughout this paper, we focus on the outer product partitioning case. In this case, we want to compute*

$$AB = \begin{bmatrix} A_1 B_1 & A_1 B_2 & \dots & A_1 B_L \\ A_2 B_1 & A_2 B_2 & \dots & A_2 B_L \\ \vdots & \vdots & \ddots & \vdots \\ A_K B_1 & A_K B_2 & \dots & A_K B_L \end{bmatrix}. \quad (19)$$

In order to ensure security for each of these matrices, a subspace with dimension at least  $T$  has to be designed to protect the transmitted matrices. For the outer product,  $AB$ , this will result in a noise space with high dimensionality. Without careful design, the resulting code may suffer rate inefficiency.

To address this, we adopt polynomial codes: Polynomial codes are considered as a special case of linear codes due to their nice structure that can be utilized in the analysis. A polynomial code for product computation is defined by two polynomials,  $f : \mathbb{F}_q \rightarrow \mathbb{F}_q^{s \times \kappa}$  and  $g : \mathbb{F}_q \rightarrow \mathbb{F}_q^{\kappa \times \ell}$ , and the goal is to compute  $h = fg$  using the  $N$  servers. Classically, once the user receives the responses,  $h$ , the required multiplication can be reconstructed, i.e.,

$$H(AB|h_{[N]}) = 0. \quad (20)$$

In addition, the rate can be defined as

$$R_C(K, L, T) = \frac{KL}{N}. \quad (21)$$

---

<sup>1</sup>It is assumed that  $A$  and  $B$  are generated independently and uniform at random.

**Remark 2** *It is important to note that, since only one polynomial,  $f$ , is used to encode the sub-blocks of  $A_i$ , sub-blocks have to be of equal dimensions, or zero padding must be used. The same argument holds for the sub-blocks of  $B$ .*

In the quantum setting, the servers share an entangled state in the quantum system  $\mathbf{Q}^{\text{init}} = \mathbf{Q}_1^{\text{init}} \cdot \mathbf{Q}_2^{\text{init}} \dots \mathbf{Q}_N^{\text{init}}$ , where the  $\mathbf{Q}_n^{\text{init}}$  subsystem is at a state represented by the density matrix  $\rho_n^{\text{init}} = \text{tr}_{j \in [N] \setminus \{n\}}(\rho^{\text{init}})$ , where  $\text{tr}_m(\cdot)$  is the partial trace operator in the finite Hilbert space defined in Section 2. The user sends the sub-blocks' encoded versions,  $f_n$  and  $g_n$ , to the  $n$ th server over a classical noiseless channel analogous to the classical PDMM protocol. Once the  $n$ th server receives the encoded versions, it can apply classical operations and encode over its own quantum state,  $\rho_n^{\text{init}}$ , to produce another quantum state  $\rho_n$ , i.e.,

$$\rho_n = \text{Enc}(\rho_n^{\text{init}}, f_n, g_n). \quad (22)$$

Then, each server transmits  $\rho_n$  to the user over a noise-free quantum channel. Upon receiving all quantum subsystems, the user applies an appropriate measurement to recover the classical output,  $Y$ , from the quantum states to decode the required multiplication,  $AB$ , i.e.,

$$H(AB|Y) = 0. \quad (23)$$

**Remark 3** *Our encoding and decoding approaches follow the  $N$ -sum-box framework described in the subsequent sections.*

The efficiency, i.e., rate, for any scheme satisfying (18) and (23) is defined as the ratio between the number of computations and the number of downloaded symbols, i.e.,

$$R(K, L, T) = \frac{mKL}{N}, \quad (24)$$

where  $m$  is an integer representing the number of instances for  $AB$  that can be computed. This is a generalization for the rate formulation; however, in the classical setting, we have  $m = 1$  and the classical rate is defined as  $R_C(K, L, T)$ . In the quantum setting,  $m = 2$ , which will become clear in later sections. The quantum rate is denoted as  $R_Q(K, L, T)$ . It is important to note that the number of servers in the quantum setting can potentially be different than the number of servers in the classical setting.

## 4 Classical and Quantum GASP<sub>r</sub> Codes

In this section, we first review the construction of the classical GASP codes, along with some of their important properties. Then, we develop the quantum version of the GASP codes. Towards constructing the quantum GASP codes, we provide a feasibility condition that needs to be satisfied. Then, we provide the encoding and decoding structure for the

quantum GASP codes once the aforementioned condition is satisfied.

## 4.1 Classical GASP<sub>r</sub> Codes

Now, we provide some conditions to ensure the decodability and privacy in polynomial codes. We then describe the classical GASP codes by defining the values of the exponents for each polynomial.

**Theorem 5 (Definition 5 and Theorem 1 in [30])** *Let  $\alpha \in \mathbb{N}^{K+T}$ ,  $\beta \in \mathbb{N}^{L+T}$ , the outer sum  $\alpha \oplus \beta$  code is decodable and  $T$ -private if*

1.  $(\alpha \oplus \beta)_{k,\ell} \neq (\alpha \oplus \beta)_{k',\ell'}, \forall (k,\ell) \in [K] \times [L], \text{ and } (k',\ell') \in [K+T] \times [L+T], (k,\ell) \neq (k',\ell'),$
2.  $\alpha_{K+t} \neq \alpha_{K+t'}, \text{ and } \beta_{L+t} \neq \beta_{L+t'}, \forall t \neq t'.$

**Definition 6 (GASP codes [30])** *Given  $K, L$  and  $T$ , for any  $1 \leq r \leq \min\{K, T\}$ , the GASP<sub>r</sub> code is defined by the following two polynomials  $f(x) = \sum_{k=1}^K A_k x^{\alpha_k} + \sum_{t=1}^T R_t x^{\alpha_{K+t}}$ , and  $g(x) = \sum_{\ell=1}^L B_\ell x^{\beta_\ell} + \sum_{t=1}^T S_t x^{\beta_{L+t}}$ , where  $A_k$  and  $B_\ell$  are the matrix partitionings,  $R_t$  and  $S_t$  are uniform noise random variables for masking, and the two polynomial exponents are chosen such that the decodability and  $T$ -privacy stated in Theorem 5 are satisfied as follows,*

$$\alpha_1 = (0, 1, \dots, K-1), \tag{25}$$

$$\alpha_2 = (KL, KL+1, \dots, KL+r-1, KL+K, KL+K+1, \dots, KL+K+r-1, \dots) \text{ of size } T, \tag{26}$$

$$\beta_1 = (0, K, \dots, K(L-1)), \tag{27}$$

$$\beta_2 = (KL, KL+1, \dots, KL+T-1), \tag{28}$$

$$\alpha = (\alpha_1, \alpha_2), \tag{29}$$

$$\beta = (\beta_1, \beta_2), \tag{30}$$

with the number of servers  $N$  satisfying  $N = |\text{Set}(\alpha \oplus \beta)|$ .

## 4.2 Generator Matrix Representation

Let  $\mathcal{S} = \text{Set}(\alpha \oplus \beta) \subset \mathbb{N}$  and fix an indexing for  $\mathcal{S}$  with  $|\mathcal{S}| = N$ . Then, the generator matrix for GASP<sub>r</sub> in a finite field  $\mathbb{F}_{q^m}$ , with  $q \geq \mathcal{S}(N)$ , can be written as

$$G_{\text{GASP}_r} = \begin{bmatrix} a_1^{\mathcal{S}} \\ \vdots \\ a_N^{\mathcal{S}} \end{bmatrix}, \tag{31}$$

where  $a_1, a_2, \dots, a_N$  are chosen uniformly at random from  $\mathcal{G} \subseteq \mathbb{F}_{q^m}$ ,  $|\mathcal{G}| > (2\binom{N}{T} + 1)J$ , with  $J = \sum_{j \in \mathcal{S}} j$ ,  $a_i^S = [a_i^{S(1)}, \dots, a_i^{S(N)}]$ , and

$$\begin{aligned} N = & KL + 2K + 3T - 2 - \max(K, \varphi) + (L - 2) \max(0, \min(r, r - \varphi)) \\ & + \left\lfloor \frac{T-1}{r} \right\rfloor \min(T-1, K-r) \\ & - \mathbb{1}_{\{\varphi < r\}} \cdot \left( \min(0, \mu - r) + r \frac{T - \mu - 1}{K} + \frac{Kx^2 + bx + T - \mu - 1}{2} \right. \\ & \quad \left. - \frac{(T - \mu - 1)(T + \mu - 1)}{2K} \right), \end{aligned} \quad (32)$$

with  $\varphi = T - 1 - KL + 2K$ ,  $\mu = (T - 1) \bmod K$ ,  $x = \min\left(\frac{T - \mu - 1}{K} - \mathbb{1}_{\{\mu=0\}}, L - 3\right)$ , and  $b = -K - 2 \max(0, \varphi) + 2T - 2$ .

**Remark 4** *A detailed proof that the generator matrix  $G$  is invertible with specific values of elements, which can be chosen prior to the scheme initiation, is provided in [30, Appendix A].*

**Remark 5** *We note that the number of servers  $N$  is also a function of  $r$ . However, we drop the function notation for simplicity if it is clear from the context.*

### 4.3 Quantum GASP<sub>r</sub> Codes

As in the previous section, we assume that the user shares a classical channel with the  $N$  servers to send the encoded versions of the sub-matrices,  $f_{[N]}$  and  $g_{[N]}$ . Upon receiving the encoded classical sub-matrices, the entangled servers apply classical and quantum operations individually, and transmit qudits back to the user over separate quantum channels. In this section, we provide the required condition such that the GASP codes can be extended to the quantum GASP codes and specify the corresponding scheme.

#### 4.3.1 Quantum GASP<sub>r</sub> Condition

In this section, to specify the feasibility condition, we first define the longest consecutive chain (LCC) function and the partitioning of any matrix generated by  $\alpha \oplus \beta$  into the information sub-space, upper left corner ( $\mathcal{UL}$ ) in the case of GASP, and interference subspace ( $\mathcal{IS}$ ).

**Definition 7** *Let  $LCC : \mathcal{X} \rightarrow \mathcal{Y}$ , where  $\mathcal{X} \subset \mathbb{N}$ , and  $\mathcal{Y} \subseteq \mathcal{X}$ . Then,  $LCC(\cdot)$  returns the longest arithmetic progression with unit difference in  $\mathcal{X}$ .*

**Definition 8** *Let  $PM$  be a matrix in  $\mathbb{N}^{K+T \times L+T}$ , such that,*

$$PM(i, j) = \alpha(i) + \beta(j), \quad (33)$$

and define  $\mathcal{UL}$  as the set

$$\mathcal{UL} = \text{Set}(PM(1 : K, 1 : L)). \quad (34)$$

The complement of  $\mathcal{UL}$  is defined as  $\mathcal{IS}$ , where

$$\mathcal{IS} = \text{Set}(PM) \setminus \mathcal{UL}. \quad (35)$$

Now, to generate a scheme for the quantum GASP, we define the feasibility constraint mentioned in the previous sections.

**Definition 9 (Feasibility constraint)** *Let  $r^*$  be the optimal parameter for  $GASP(K, L, T)$  with the optimal number of servers  $N_{GASP}^*(K, L, T)$ . Define  $PM$  as above with  $\alpha$  and  $\beta$  based on  $r^*$ . Then, the feasibility constraint is defined as*

$$|LCC(\mathcal{IS})| \geq \left\lceil \frac{N_{GASP}^*(K, L, T)}{2} \right\rceil. \quad (36)$$

**Theorem 6 (Quantum GASP<sub>r</sub>)** *Given  $K$ ,  $L$  and  $T$ , let  $N_{GASP}^*(K, L, T)$  be the optimal number of servers for the GASP codes. If (36) is satisfied, then there exists a quantum coding scheme for PDMM such that the rate is*

$$R_Q = \frac{2KL}{N_{GASP}^*(K, L, T)}. \quad (37)$$

In order to quantify the applicability of the feasibility condition (36), we provide an estimate for the least value of the privacy parameter needed in order to extend the classical GASP codes to the quantum GASP. Since there is no closed-form solution for the optimal number of servers for GASP, we provide numerical representations with figures. Fig. 3 shows that in the case of  $K = L$ , as  $K$  increases, the minimum value of  $T$  required to satisfy the feasibility constraint increases quadratically in the following way to the nearest integer

$$\hat{T} = 0.5K^2 - 10^{-3}K + 0.772. \quad (38)$$

To move from the  $K = L$  case to the  $K \geq L$  case, Fig. 4 shows the 3D plot relating the 3 variables. It can be estimated, using multi-variable regression up to quadratic terms, as

$$\hat{T} = -0.043L^2 + 0.507KL + 0.18K + 0.362L - 0.746. \quad (39)$$

The  $R^2$  score (which explains the percentage of variation in the output that the model can explain) in this case is 0.998. Although the  $R^2$  score is high and the estimate of the case when  $K = L$  matches well with the real curve, these relations are empirical approximations based on the specified parameter range.

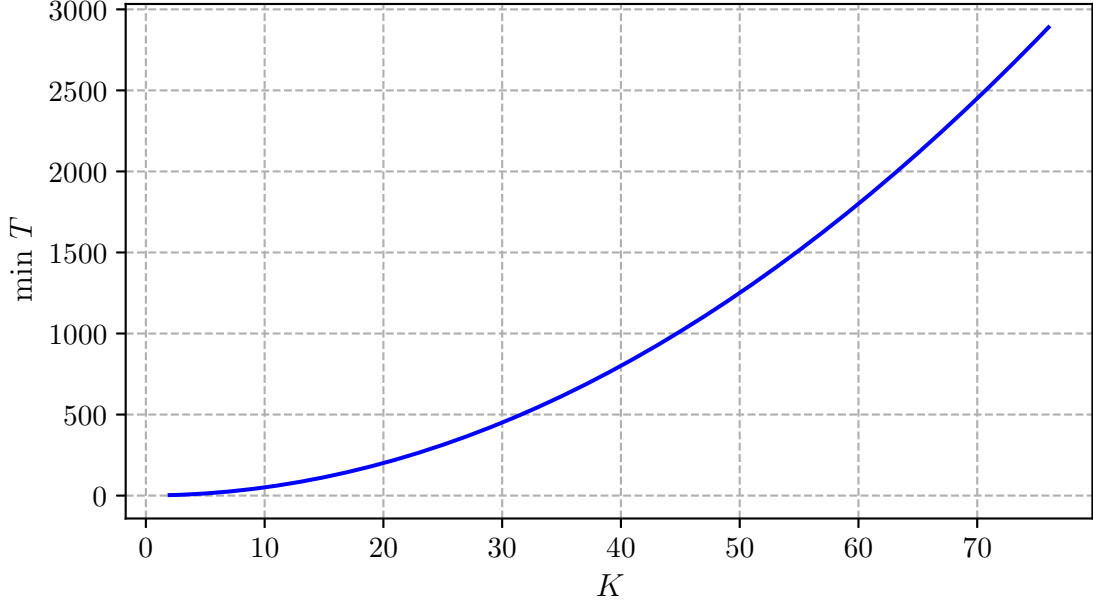


Figure 3: Min  $T$  needed for  $K = L$  to satisfy (36).

#### 4.3.2 Quantum GASP Scheme

We now present the details of the proposed quantum GASP scheme. The user sends the two polynomials  $f(x)$  and  $g(x)$  defined as

$$f(a_i) = \sum_{k=1}^K A_k a_i^{\alpha_k} + \sum_{t=1}^T R_t a_i^{\alpha_{K+t}}, \quad (40)$$

$$g(a_i) = \sum_{\ell=1}^L B_\ell a_i^{\beta_\ell} + \sum_{t=1}^T S_t a_i^{\beta_{L+t}}, \quad (41)$$

to each of the  $N$  servers. Upon receiving them, each server applies the multiplication and computes

$$F^{[m]}(a_n) = \sum_{k \in [K], \ell \in [L]} A_k^{[m]} B_\ell^{[m]} a_n^{(\alpha \oplus \beta)_{k,\ell}} + \sum_{(i,j) \in \mathcal{Q}} I_{i,j}^{[m]} a_n^{(\alpha \oplus \beta)_{i,j}}, \quad m \in [2], \quad (42)$$

where  $\mathcal{Q} = \{(i, j) : i \in [K + T], j \in [L + T], (i, j) \notin ([K], [L])\}$ .

Let  $i_{k,\ell} = (\alpha \oplus \beta)_{k,\ell}$ . Thus, for every  $(k, \ell) \in [K] \times [L]$ ,  $i_{k,\ell} \in \mathcal{UL}$ . Similarly, for every  $(i, j) \in \mathcal{Q}$ , we represent  $(\alpha \oplus \beta)_{i,j}$  as  $c_{i,j}$  and  $c_{i,j} \in \mathcal{IS}$ . Thus, (42) can be written as

$$F^{[m]}(a_n) = \sum_{i_{k,\ell} \in \mathcal{UL}} A_k^{[m]} B_\ell^{[m]} a_n^{i_{k,\ell}} + \sum_{c_{i,j} \in \mathcal{IS}} I_{c_{i,j}}^{[m]} a_n^{c_{i,j}} \quad (43)$$

$$= \sum_{i_{k,\ell} \in \mathcal{UL}} A_k^{[m]} B_\ell^{[m]} a_n^{i_{k,\ell}} + \sum_{c_{i,j} \in \mathcal{IS} \setminus \text{LCC}(\mathcal{IS})} I_{c_{i,j}}^{[m]} a_n^{c_{i,j}} + \sum_{c_{i,j} \in \text{LCC}(\mathcal{IS})} I_{c_{i,j}}^{[m]} a_n^{c_{i,j}}, \quad m \in [2]. \quad (44)$$



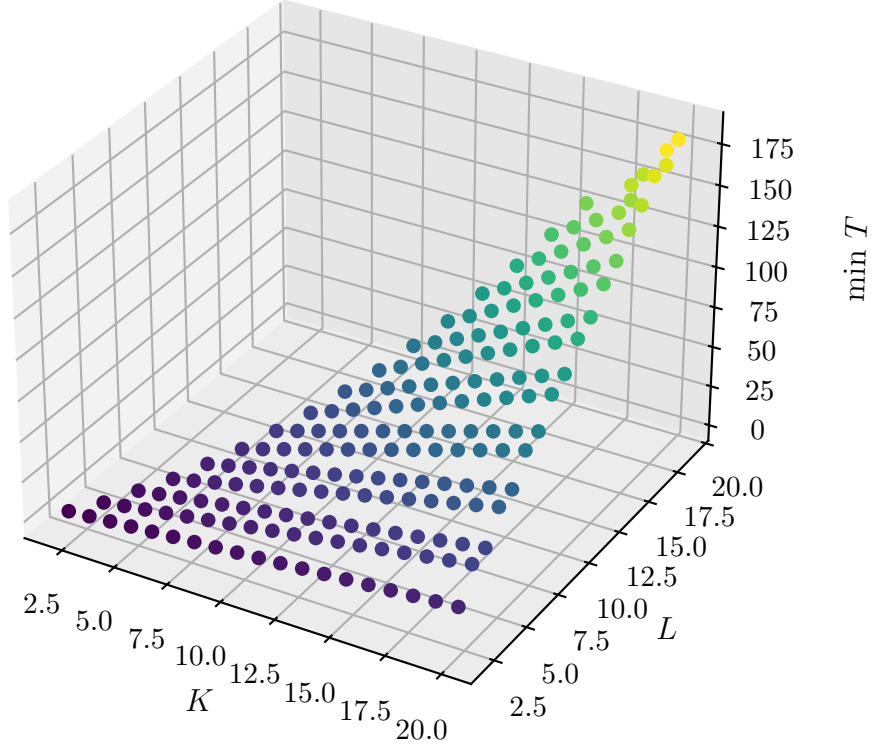


Figure 4: Min  $T$  needed for  $K$  and  $L$  to satisfy (36).

To make the notation easy, first we define  $\mathcal{S} = \text{LCC}(\mathcal{IS})$ , and  $\mathcal{R} = \mathcal{IS} \setminus \text{LCC}(\mathcal{IS})$ . In addition, note that the running index pair  $(i, j)$  for the interference terms can be substituted by  $\mathcal{S}$  and  $\mathcal{R}$  as follows

$$F^{[m]}(a_n) = \sum_{i_{k,\ell} \in \mathcal{UL}} A_k^{[m]} B_\ell^{[m]} a_n^{i_{k,\ell}} + \sum_{\substack{r_i \in \mathcal{R}: \\ i \in [|\mathcal{R}|]}} I_{r_i}^{[m]} a_n^{r_i} + \sum_{\substack{s_i \in \mathcal{S}: \\ i \in [|\mathcal{S}|]}} I_{s_i}^{[m]} a_n^{s_i}, \quad m \in [2]. \quad (45)$$

Now, for each element in  $F_n^{[1]} = F^{[1]}(a_n)$ ,  $F_n^{[2]} = F^{[2]}(a_n)$ , the server applies Pauli operators on each element as follows

$$\mathbf{X}(u_n F_n^{[1]}(i, j)) \mathbf{Z}(v_n F_n^{[2]}(i, j)) \rho_n \mathbf{X}^\dagger(u_n F_n^{[1]}(i, j)) \mathbf{Z}^\dagger(v_n F_n^{[2]}(i, j)). \quad (46)$$

Let us denote the optimal number of servers as  $N^*$  for ease of notation. Thus, the transmitted

symbols for each  $(i, j)$  is given by

$$X(i, j) = \begin{bmatrix} F_1^{[1]}(i, j) \\ \vdots \\ F_{N^*}^{[1]}(i, j) \\ F_1^{[2]}(i, j) \\ \vdots \\ F_{N^*}^{[2]}(i, j) \end{bmatrix} \quad (47)$$

$$= \begin{bmatrix} \text{diag}(u)G_{\text{GASP}_{N^*}} & 0_{N^*} \\ 0_{N^*} & \text{diag}(v)G_{\text{GASP}_{N^*}} \end{bmatrix} \times \left[ (A_1 B_1)^{[1]}(i, j), \dots, (A_K B_L)^{[1]}(i, j), I_1^{[1]}(i, j), \dots, I_{N^*-KL}^{[1]}(i, j), (A_1 B_1)^{[2]}(i, j), \dots, (A_K B_L)^{[2]}(i, j), I_1^{[2]}(i, j), \dots, I_{N^*-KL}^{[2]}(i, j) \right]^t \quad (48)$$

$$= D \begin{bmatrix} Q & 0 \\ 0 & Q \end{bmatrix} \times \left[ I_{s_1}^{[1]}(i, j), I_{s_2}^{[1]}(i, j), \dots, I_{s_{|S|}}^{[1]}(i, j), (A_1 B_1)^{[1]}(i, j), \dots, (A_K B_L)^{[1]}(i, j), I_{r_1}^{[1]}(i, j), \dots, I_{r_{|\mathcal{R}|}}^{[1]}(i, j), I_{s_1}^{[2]}(i, j), I_{s_2}^{[2]}(i, j), \dots, I_{s_{|S|}}^{[2]}(i, j), (A_1 B_1)^{[2]}(i, j), \dots, (A_K B_L)^{[2]}(i, j), I_{r_1}^{[2]}(i, j), \dots, I_{r_{|\mathcal{R}|}}^{[2]}(i, j) \right]^t, \quad (49)$$

where  $D = \begin{bmatrix} \text{diag}(u) & 0_{N^*} \\ 0_{N^*} & \text{diag}(v) \end{bmatrix}$ , and

$$Q = \begin{bmatrix} a_1^{s_1} & a_1^{s_2} & \dots & a_1^{s_{|S|}} & a_1^{i_{1,1}} & a_1^{i_{1,2}} & \dots & a_1^{i_{K,L}} & a_1^{r_1} & \dots & a_1^{r_{|\mathcal{R}|}} \\ a_2^{s_1} & a_2^{s_2} & \dots & a_2^{s_{|S|}} & a_2^{i_{1,1}} & a_2^{i_{1,2}} & \dots & a_2^{i_{K,L}} & a_2^{r_1} & \dots & a_2^{r_{|\mathcal{R}|}} \\ \vdots & \vdots & \ddots & \vdots & \vdots & \vdots & \ddots & \vdots & \vdots & \ddots & \vdots \\ a_{N^*}^{s_1} & a_{N^*}^{s_2} & \dots & a_{N^*}^{s_{|S|}} & a_{N^*}^{i_{1,1}} & a_{N^*}^{i_{1,2}} & \dots & a_{N^*}^{i_{K,L}} & a_{N^*}^{r_1} & \dots & a_{N^*}^{r_{|\mathcal{R}|}} \end{bmatrix} \quad (50)$$

$$= \begin{bmatrix} a_1^s & a_1^{s+1} & \dots & a_1^{s+|S|-1} & a_1^{i_{1,1}} & a_1^{i_{1,2}} & \dots & a_1^{i_{K,L}} & a_1^{r_1} & \dots & a_1^{r_{|\mathcal{R}|}} \\ a_2^s & a_2^{s+2} & \dots & a_2^{s+|S|-1} & a_2^{i_{1,1}} & a_2^{i_{1,2}} & \dots & a_2^{i_{K,L}} & a_2^{r_1} & \dots & a_2^{r_{|\mathcal{R}|}} \\ \vdots & \vdots & \ddots & \vdots & \vdots & \vdots & \ddots & \vdots & \vdots & \ddots & \vdots \\ a_{N^*}^s & a_{N^*}^{s+1} & \dots & a_{N^*}^{s+|S|-1} & a_{N^*}^{i_{1,1}} & a_{N^*}^{i_{1,2}} & \dots & a_{N^*}^{i_{K,L}} & a_{N^*}^{r_1} & \dots & a_{N^*}^{r_{|\mathcal{R}|}} \end{bmatrix}. \quad (51)$$

We next design a transfer matrix  $M$  that satisfies the requirements in Theorem 4. Accordingly, we construct the following matrix and show that it satisfies the required properties

$$M = \begin{bmatrix} 0 & I_{N^*} \end{bmatrix} \begin{bmatrix} G & H \end{bmatrix}^{-1}, \quad (52)$$

where

$$G = \begin{bmatrix} DQ(:, 1 : \lfloor \frac{N^*}{2} \rfloor) & 0 \\ 0 & DQ(:, 1 : \lceil \frac{N^*}{2} \rceil) \end{bmatrix}, \quad (53)$$

and

$$H = \begin{bmatrix} DQ(:, \lfloor \frac{N^*}{2} \rfloor + 1 : N^*) & 0 \\ 0 & DQ(:, \lceil \frac{N^*}{2} \rceil + 1 : N^*) \end{bmatrix}. \quad (54)$$

Consequently, the received symbols are given by

$$\begin{aligned} Y(i, j) = MX(i, j) = & \left[ I_{s_{\lfloor \frac{N^*}{2} \rfloor + 1}}^{[1]}(i, j), \dots, I_{s_{|S|}}^{[1]}(i, j), (A_1 B_1)^{[1]}(i, j), \dots, (A_K B_L)^{[1]}(i, j), \right. \\ & I_{r_1}^{[1]}(i, j), \dots, I_{r_{|\mathcal{R}|}}^{[1]}(i, j), I_{s_{\lceil \frac{N^*}{2} \rceil + 1}}^{[2]}(i, j), \dots, I_{s_{|S|}}^{[2]}(i, j), \\ & \left. (A_1 B_1)^{[2]}(i, j), \dots, (A_K B_L)^{[2]}(i, j), I_{r_1}^{[2]}(i, j), \dots, I_{r_{|\mathcal{R}|}}^{[2]}(i, j) \right]^t. \end{aligned} \quad (55)$$

As shown, the scheme provides 2 instances in each  $N^*$  qubits transmission compared to one instance for the classical counterpart. Thus, the rate is given by  $R_Q = 2R_C$ .

Now, we need to show that the chosen  $\begin{bmatrix} G & H \end{bmatrix}$  satisfies the requirements in Theorem 4. First, it follows directly that

$$\begin{bmatrix} \text{diag}(u)G_{\text{GASP}_{N^*}} & 0_{N^*} \\ 0_{N^*} & \text{diag}(v)G_{\text{GASP}_{N^*}} \end{bmatrix} \quad (56)$$

is invertible if  $G_{\text{GASP}}$  is invertible. Since applying any column permutation will not affect the span of the column space, the required matrix is invertible.

Finally, we verify that  $G$  is an SSO matrix.

$$\begin{aligned} G = & \begin{bmatrix} DQ(:, 1 : \lfloor \frac{N^*}{2} \rfloor) & 0 \\ 0 & DQ(:, 1 : \lceil \frac{N^*}{2} \rceil) \end{bmatrix} \\ = & \begin{bmatrix} \text{diag}(u) & 0_{N^*} \\ 0_{N^*} & \text{diag}(v) \end{bmatrix} \begin{bmatrix} a_1^s & a_1^{s+1} & \dots & a_1^{s+\lfloor \frac{N^*}{2} \rfloor-1} & 0 & 0 & \dots & 0 \\ a_2^s & a_2^{s+1} & \dots & a_2^{s+\lfloor \frac{N^*}{2} \rfloor-1} & 0 & 0 & \dots & 0 \\ \vdots & \vdots & \ddots & \vdots & \vdots & \vdots & \ddots & \vdots \\ a_{N^*}^s & a_{N^*}^{s+1} & \dots & a_{N^*}^{s+\lfloor \frac{N^*}{2} \rfloor-1} & 0 & 0 & \dots & 0 \\ 0 & 0 & \dots & 0 & a_1^s & a_1^{s+1} & \dots & a_1^{s+\lceil \frac{N^*}{2} \rceil-1} \\ 0 & 0 & \dots & 0 & a_2^s & a_2^{s+1} & \dots & a_2^{s+\lceil \frac{N^*}{2} \rceil-1} \\ \vdots & \vdots & \ddots & \vdots & \vdots & \vdots & \ddots & \vdots \\ 0 & 0 & \dots & 0 & a_{N^*}^s & a_{N^*}^{s+1} & \dots & a_{N^*}^{s+\lceil \frac{N^*}{2} \rceil-1} \end{bmatrix}. \end{aligned} \quad (58)$$

To prove that  $G$  satisfies the SSO condition if  $u$  and  $v$  are chosen to generate dual codes, we provide the following theorem.

**Theorem 7** *Let  $G = \begin{bmatrix} M_{n \times k} & 0_{n \times n-k} \\ 0_{n \times k} & S_{n \times n-k} \end{bmatrix}$ . If  $M$  and  $S$  are generators of two dual codes, then  $G$  satisfies the SSO condition.*

The proof of the theorem is done by just computing the value of  $G^t J G$  in terms of  $M$  and  $S$ , recalling that they are dual. Thus,  $G^t J G = 0$  is satisfied when the values of  $u$  and  $v$  are chosen so that the shifted GRS codes are dual.

## 4.4 Discussion and Further Remarks

Two potential research directions emerge from the results presented in this section. The first is to investigate alternative methods for constructing dual codes for the GASP, that relax the feasibility requirement in (36). The other approach is to consider all possible  $r$  given  $K$ ,  $L$  and  $T$ . This might give more possibilities for satisfying the feasibility constraint in (36) with acceptable sub-optimality.

From the  $\hat{T}$  estimate relation for  $K \geq L$  in (39), we can see that  $T$  is affected more by varying  $L$  than  $K$ , consequently if  $L$  can be maintained to be small, then it is possible to easily satisfy the feasibility constraint (36). Therefore, it follows that the feasibility constraint (36) is not satisfied when  $T < L$ , hence  $\text{GASP}_r$  can be extended only when  $T \geq L$ .

To address these limitations that arise from directly extending the GASP codes to the quantum setting, we develop codes in the next section, that are designed specifically for the quantum setting.

# 5 A Family of Codes for Quantum PDMM Computations in High Privacy Regime

In this section, we develop new codes for the high privacy regime. These codes do not have to satisfy the feasibility condition of GASP.

## 5.1 Main Results

**Theorem 8** *Let  $K = L = T = n^2$ , then there exists a quantum scheme based on a polynomial code that achieves a rate equal to*

$$R_Q(n^2, n^2, n^2) = \frac{2n^4}{2n^4 + 2n^2 - 1}. \quad (59)$$

**Theorem 9** *Let  $K = L = n^k$ , and  $T = n^m$ , with  $m \geq k \geq 2$ , then there exists a quantum scheme based on a polynomial code that achieves a rate equal to*

$$R_Q(n^k, n^k, n^m) = \frac{2n^{2k}}{2n^{2k} + 3n^m - n^k - 1}. \quad (60)$$

**Corollary 1** *Let  $K = L = n^2$  and  $T = n^3$ , then there exists a quantum scheme based on a polynomial code that achieves a rate equal to*

$$R_Q(n^2, n^2, n^3) = \frac{2n^4}{2n^4 + 3n^3 - n^2 - 1}. \quad (61)$$

**Corollary 2** *Let  $K = L = n^2$  and  $T = n^4$ , then there exists a quantum scheme based on a polynomial code that achieves a rate equal to*

$$R_Q(n^2, n^2, n^4) = \frac{2n^4}{5n^4 - n^2 - 1}. \quad (62)$$

**Remark 6** *Although Theorem 8 is a special case of Theorem 9, it is presented separately for clarity of comparison. The former is the only closed-form solution for the number of servers in the main GASP paper [45]. Thus, we consider it a stand-alone result.*

**Theorem 10** *Let  $K = L = n^k$ , and  $T = n^k + r$ , with  $0 \leq r < n^{2k} - n^k + 1$ , then there exists a quantum scheme based on a polynomial code that achieves a rate equal to*

$$R_Q(n^k, n^k, n^k + r) = \frac{2n^{2k}}{2n^{2k} + 2n^k + 2r - 1}. \quad (63)$$

**Theorem 11** *For  $K \geq L = T$ , then there exists a quantum scheme based on the polynomial code that achieves a rate equal to*

$$R_Q(K, L, T) = \frac{2KT}{2KT + 2T - 1}. \quad (64)$$

**Corollary 3** *Let  $K = 3$ ,  $L = 2$  and  $T = 2$ , then there exists a quantum scheme based on a polynomial code that achieves a rate equal to*

$$R_Q(3, 2, 2) = 0.8, \quad (65)$$

*and we have the following ratio*

$$\frac{R_Q(3, 2, 2)}{R_C(3, 2, 2)} = 1.87. \quad (66)$$

**Corollary 4** *Let  $K = 4$ ,  $L = T = 2$ , then there exists a quantum scheme based on a*

polynomial code that achieves a rate equal to

$$R_Q(4, 2, 2) = \frac{16}{19}, \quad (67)$$

and we have the following ratio

$$\frac{R_Q(4, 2, 2)}{R_C(4, 2, 2)} = 1.8. \quad (68)$$

**Corollary 5** *Let  $K = 6$ ,  $L = T = 2$ , then there exists a quantum scheme based on a polynomial code that achieves a rate equal to*

$$R_Q(6, 2, 2) = \frac{24}{27}, \quad (69)$$

and we have the following ratio

$$\frac{R_Q(6, 2, 2)}{R_C(6, 2, 2)} = 1.7. \quad (70)$$

**Theorem 12** *Let  $K = T = n^k$  and  $L = n^\ell$  with  $k \geq \ell$ , then there exists a quantum scheme based on a polynomial code that achieves a rate equal to*

$$R_Q(n^k, n^\ell, n^k) = \frac{2n^{k+\ell}}{2n^{k+\ell} + 2n^k - 1}. \quad (71)$$

**Corollary 6** *Let  $K = T = 2^3$  and  $L = 2$ , then*

$$\frac{R_Q(8, 2, 8)}{R_C(8, 2, 8)} = 2. \quad (72)$$

**Theorem 13** *Let  $K = T = n^\ell + r$  and  $L = n^\ell$  with  $r > 0$ , then there exists a quantum scheme based on a polynomial code that achieves a rate equal to*

$$R_Q(n^\ell + r, n^\ell, n^\ell + r) = \frac{2n^{2\ell} + 2rn^\ell}{2n^{2\ell} + 2rn^\ell + 2n^\ell + 2r - 1}. \quad (73)$$

**Remark 7** *Note the difference between Theorems 9 and 12 where the first is when  $K = L$ , and the latter is  $K = T$ . Similarly, for Theorems 10 and 13.*

**Remark 8** *Although Theorem 13 is a general case of Theorem 12, when substituting  $r = n^k - n^\ell$ , the number of required servers is more in the latter compared to the former, which decreases the rate. Thus, the designed code for the special case in Theorem 12 is more optimized than the general one in Theorem 13. It is exactly the same case for Theorem 9 and Theorem 10.*

**Remark 9** *All the rate comparisons here are with respect to the classical GASP scheme.*

As mentioned earlier, Theorem 8 is the only theorem that we can compare analytically with the GASP code since it is the only closed-form result. First, let us recall the GASP code result for the same setting.

**Theorem 14 (Proposition 1 in [45])** *For  $K = L = T = n^2$ , the optimal rate for GASP when  $n > 1$  is given by*

$$R_C(n^2, n^2, n^2) = \frac{n^4}{n^4 + 2n^3 + 2n^2 - n - 2}. \quad (74)$$

Thus, the ratio between the classical and the quantum schemes in this case is given by

$$\frac{R_Q(n^2, n^2, n^2)}{R_C(n^2, n^2, n^2)} = \frac{2n^4 + 4n^3 + 4n^2 - 2n - 4}{2n^4 + 2n^2 - 1}. \quad (75)$$

In comparison with the classical GASP, Figs. 5-9 are plotted to compare for the cases of Theorems 9 and 12. We chose both specifically since one of them has  $T$  greater than both  $K$  and  $L$ , while the other has  $T$  equal to  $K$  and greater than  $L$ . In the first case, Figs. 7, 8, and 9, show that the efficiency of our scheme increases monotonically with  $T$  until  $T = KL$ , with fixed  $K$  and  $L$ . The efficiency always goes to 1 in the case when  $T = o(KL)$  since the classical GASP scheme is optimal in the asymptotic sense. However, as  $T$  increases, our scheme becomes more efficient than the GASP code even in the asymptotic sense and achieves the highest efficiency when  $T = KL$ . In addition, in Figs. 7 and 8, the schemes developed can be unnecessary once  $m = 2k$  since the feasibility condition is then definitely satisfied, thus achieving the super-dense coding gain. Figs. 7 and 8 show that whenever  $L$  increases, the rate gain diminishes for fixed  $K = T$ .

## 5.2 Coding Schemes

In this section, we provide the exponents required for each transmitted polynomial and the encoding of the polynomials for the corresponding code so that the information subspace and the interference subspace become clear for each setting in the previous section. The transfer matrices for all these settings follow the same structure; thus, the transfer matrix and the corresponding encoding are provided only for the first setting. It can be proven that all these matrices satisfy the required properties defined in Theorem 4. In all the following regimes, we assume that the transfer matrices are in the form of

$$M = \begin{bmatrix} 0 & I_N \end{bmatrix} \begin{bmatrix} G & H \end{bmatrix}^{-1}, \quad (76)$$

and it can be shown that the chosen  $G$  and  $H$  satisfy the required conditions in Theorem 4. In addition, we denote  $\alpha = (\alpha_1, \alpha_2)$  and  $\beta = (\beta_1, \beta_2)$ .

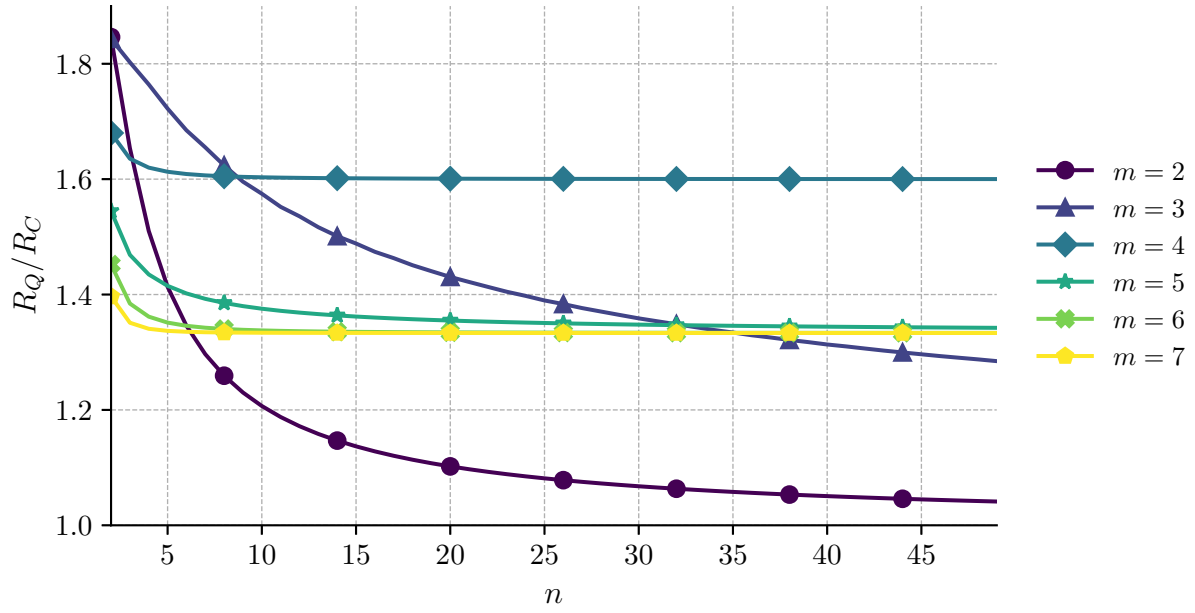


Figure 5:  $K = L = n^2$  and  $T = n^m$ , for  $m = [2 : 7]$ .

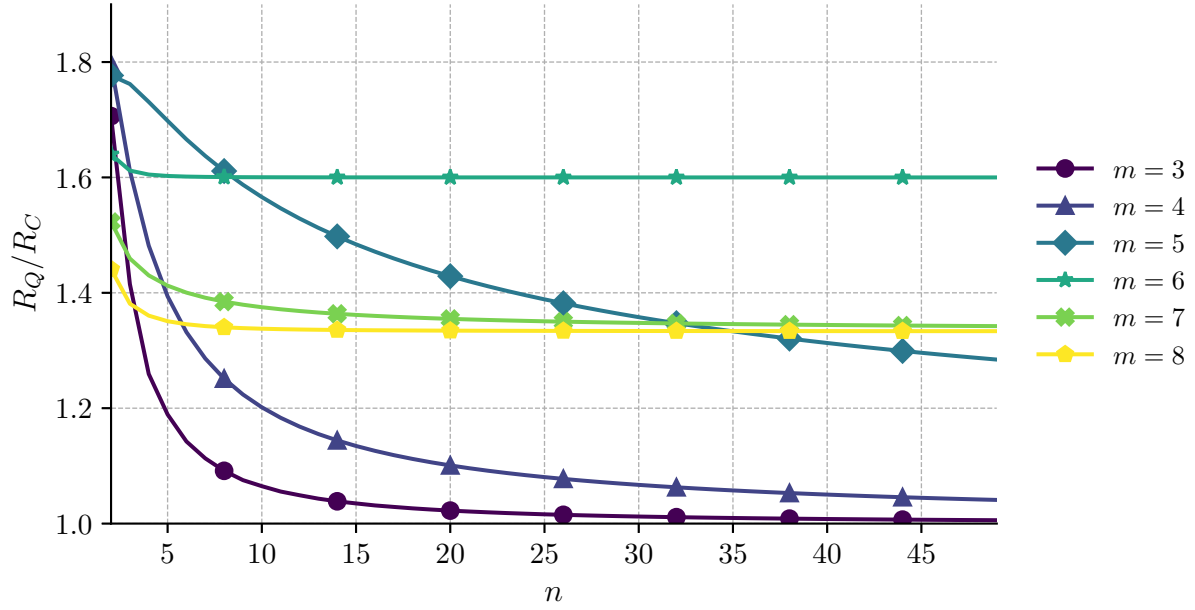


Figure 6:  $K = L = n^3$  and  $T = n^m$ , for  $m = [3 : 8]$ .



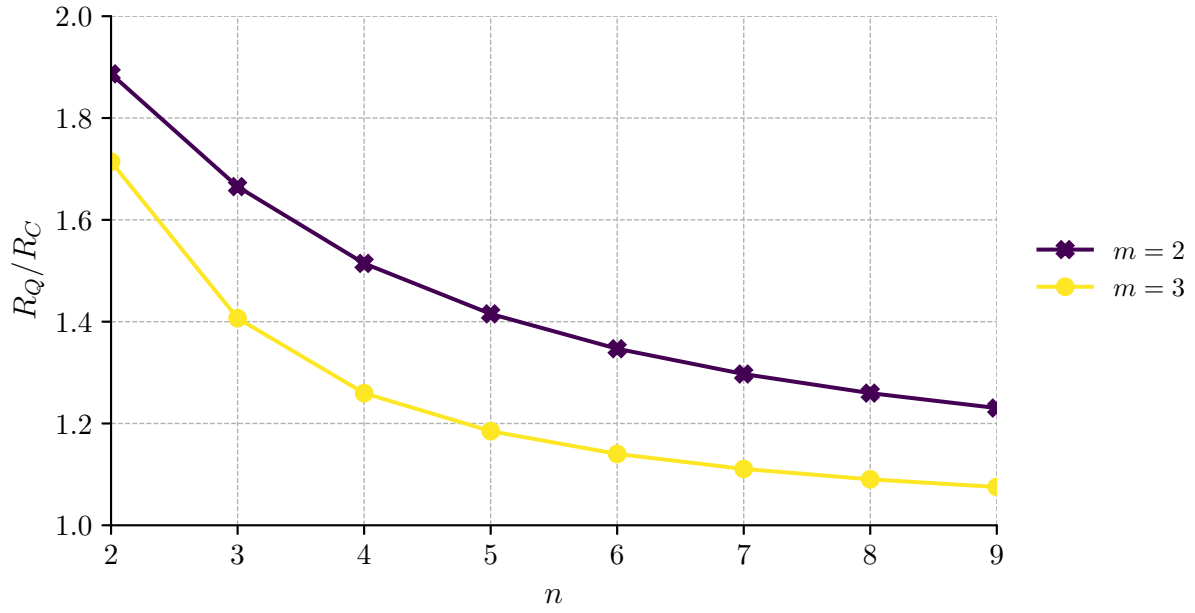


Figure 7:  $K = T = n^4$  and  $L = n^m$ , for  $m = 2, 3$ .

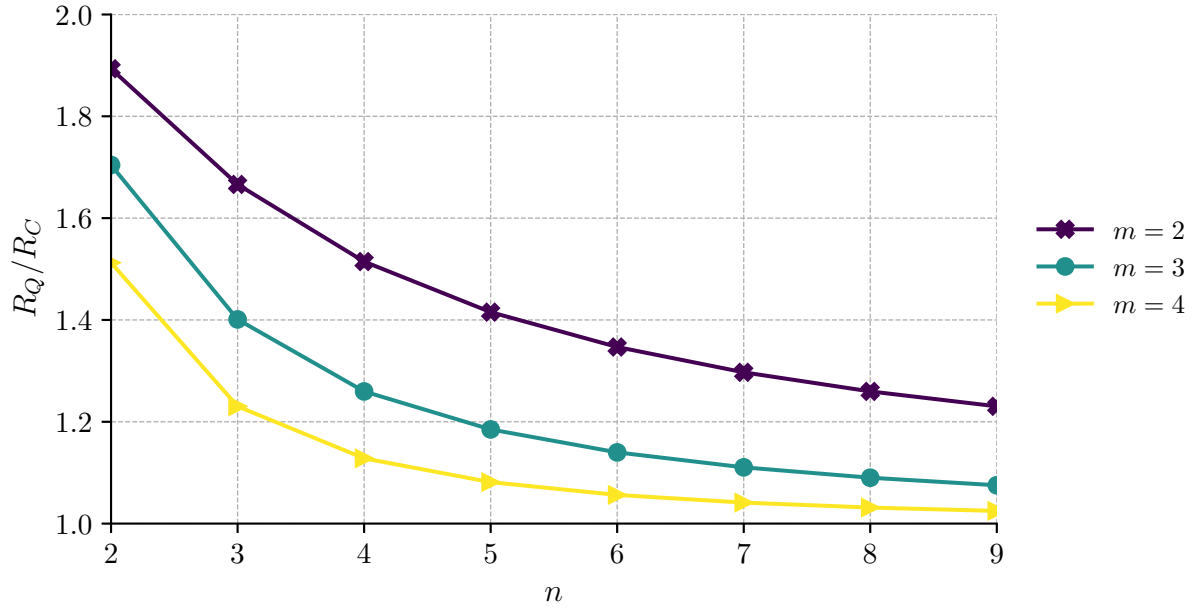


Figure 8:  $K = T = n^5$  and  $L = n^m$ , for  $m = [2 : 4]$ .

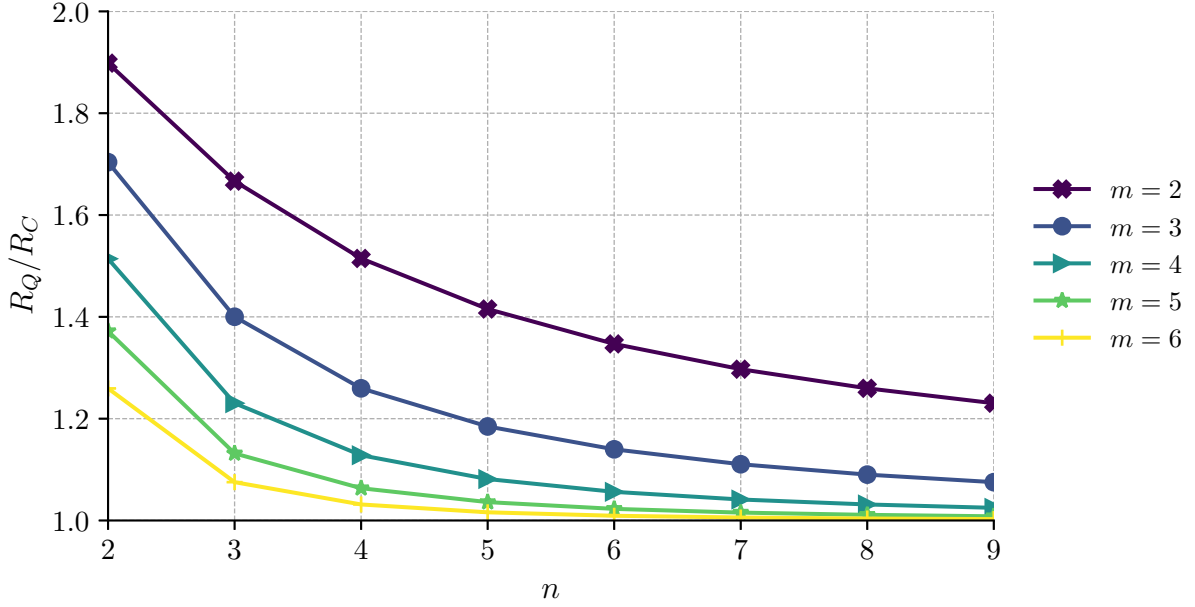


Figure 9:  $K = T = n^7$  and  $L = n^m$ , for  $m = [2 : 6]$ .

### 5.2.1 $K = L = T = n^2$

The following are the exponents, and the corresponding degree table is given in Table 1,

$$\alpha_1 = \beta_1 = [0, 1, \dots, n^2 - 1], \quad (77)$$

$$\alpha_2 = [n^4, n^4 + 1, \dots, n^4 + n^2 - 1], \quad (78)$$

$$\beta_2 = [2n^2 - 1, 3n^2 - 1, \dots, n^4 + n^2 - 1]. \quad (79)$$

$\alpha \backslash \beta$	0	1	$\dots$	$n^2 - 1$	$2n^2 - 1$	$3n^2 - 1$	$\dots$	$n^4 + n^2 - 1$
0	0	1	$\dots$	$n^2 - 1$	$2n^2 - 1$	$3n^2 - 1$	$\dots$	$n^4 + n^2 - 1$
1	1	2	$\dots$	$n^2$	$2n^2$	$3n^2$	$\dots$	$n^4 + n^2$
$\vdots$	$\vdots$	$\vdots$	$\ddots$	$\vdots$	$\vdots$	$\vdots$	$\ddots$	$\vdots$
$n^2 - 1$	$n^2 - 1$	$n^2$	$\dots$	$2n^2 - 2$	$3n^2 - 2$	$4n^2 - 2$	$\dots$	$n^4 + 2n^2 - 2$
$n^4$	$n^4$	$n^4 + 1$	$\dots$	$n^4 + n^2 - 1$	$n^4 + 2n^2 - 1$	$n^4 + 3n^2 - 1$	$\dots$	$2n^4 + n^2 - 1$
$n^4 + 1$	$n^4 + 1$	$n^4 + 2$	$\dots$	$n^4 + n^2$	$n^4 + 2n^2$	$n^4 + 3n^2$	$\dots$	$2n^4 + n^2$
$\vdots$	$\vdots$	$\vdots$	$\ddots$	$\vdots$	$\vdots$	$\vdots$	$\ddots$	$\vdots$
$n^4 + n^2 - 1$	$n^4 + n^2 - 1$	$n^4 + n^2$	$\dots$	$n^4 + 2n^2 - 2$	$n^4 + 3n^2 - 2$	$n^4 + 4n^2 - 2$	$\dots$	$2n^4 + 2n^2 - 2$

Table 1: Degree table for  $K = L = T = n^2$ .

The encoding is done as follows,

$$f(x) = \sum_{i=1}^{n^2} R_i x^{\alpha(i)} + \sum_{i=1}^{n^2} A_i x^{\alpha(i+n^2)}, \quad (80)$$

$$g(x) = \sum_{i=1}^{n^2} Z_i x^{\beta(i)} + \sum_{i=1}^{n^2} B_i x^{\beta(i+n^2)}. \quad (81)$$

As an illustrative example, we provide a detailed derivation of the transmitted and received symbols along with the chosen transfer matrix. The remaining schemes follow the same structure. The transmitted symbols can be written in the same form as the quantum GASP, with minor modifications as follows,

$$\begin{aligned} X(i, j) &= \begin{bmatrix} F_1^{[1]}(i, j) \\ \vdots \\ F_{2n^4+2n^2-1}^{[1]}(i, j) \\ F_1^{[2]}(i, j) \\ \vdots \\ F_{2n^4+2n^2-1}^{[2]}(i, j) \end{bmatrix} \\ &= \begin{bmatrix} \text{diag}(u)G' & 0_{2n^4+2n^2-1} \\ 0_{2n^4+2n^2-1} & \text{diag}(v)G' \end{bmatrix} \\ &\times \left[ I_1^{[1]}(i, j), \dots, I_{n^4+2n^2-1}^{[1]}(i, j), (A_1 B_1)^{[2]}(i, j), (A_1 B_1)^{[1]}(i, j), \dots, (A_K B_L)^{[1]}(i, j), \right. \\ &\quad \left. I_1^{[2]}(i, j), \dots, I_{n^4+2n^2-1}^{[2]}(i, j), (A_1 B_1)^{[1]}(i, j), \dots, (A_K B_L)^{[2]}(i, j) \right]^t, \end{aligned} \quad (82)$$

where

$$G' = \begin{bmatrix} 1 & a_1 & a_1^2 & \dots & a_1^{2n^4+2n^2-2} \\ 1 & a_2 & a_2^2 & \dots & a_2^{2n^4+2n^2-2} \\ \vdots & \vdots & \vdots & \ddots & \vdots \\ 1 & a_{2n^4+2n^2-1} & a_{2n^4+2n^2-1}^2 & \dots & a_{2n^4+2n^2-1}^{2n^4+2n^2-2} \end{bmatrix}. \quad (84)$$

The received symbols can be written as,

$$Y(i, j) = M X(i, j) \quad (85)$$

$$\begin{aligned} &= \left[ I_{\lfloor \frac{2n^4+2n^2-1}{2} \rfloor}^{[1]}(i, j), \dots, I_{n^4+2n^2-1}^{[1]}(i, j), (A_1 B_1)^{[1]}(i, j), \dots, (A_{n^2} B_{n^2})^{[1]}(i, j), \right. \\ &\quad \left. I_{\lceil \frac{2n^4+2n^2-1}{2} \rceil}^{[2]}(i, j), \dots, I_{n^4+2n^2-1}^{[2]}(i, j), (A_1 B_1)^{[2]}(i, j), \dots, (A_{n^2} B_{n^2})^{[2]}(i, j) \right]^t, \end{aligned} \quad (86)$$

where  $M = \begin{bmatrix} 0 & I_N \end{bmatrix} \begin{bmatrix} G & H \end{bmatrix}^{-1}$ , with

$$G = D \begin{bmatrix} 1 & a_1 & \dots & a_1^{\lfloor \frac{2n^4+2n^2-1}{2} \rfloor - 1} & 0 & 0 & \dots & 0 \\ \vdots & \vdots & \ddots & \vdots & \vdots & \vdots & \ddots & \vdots \\ 1 & a_{2n^4+2n^2-1} & \dots & a_{2n^4+2n^2-1}^{\lfloor \frac{2n^4+2n^2-1}{2} \rfloor - 1} & 0 & 0 & \dots & 0 \\ 0 & 0 & \dots & 0 & 1 & a_1 & \dots & a_1^{\lceil \frac{2n^4+2n^2-1}{2} \rceil - 1} \\ \vdots & \vdots & \ddots & \vdots & \vdots & \vdots & \ddots & \vdots \\ 0 & 0 & \dots & 0 & 1 & a_{2n^4+2n^2-1} & \dots & a_{2n^4+2n^2-1}^{\lceil \frac{2n^4+2n^2-1}{2} \rceil - 1} \end{bmatrix}, \quad (87)$$

and

$$H = D \begin{bmatrix} a_1^{\lfloor \frac{2n^4+2n^2-1}{2} \rfloor} & a_1^{\lfloor \frac{2n^4+2n^2-1}{2} \rfloor + 1} & \dots & a_1^{2n^4+2n^2-2} & 0 & 0 & \dots & 0 \\ \vdots & \vdots & \ddots & \vdots & \vdots & \vdots & \ddots & \vdots \\ a_{2n^4+2n^2-1}^{\lfloor \frac{2n^4+2n^2-1}{2} \rfloor} & a_{2n^4+2n^2-1}^{\lfloor \frac{2n^4+2n^2-1}{2} \rfloor + 1} & \dots & a_{2n^4+2n^2-1}^{2n^4+2n^2-2} & 0 & 0 & \dots & 0 \\ 0 & 0 & \dots & 0 & a_1^{\lceil \frac{2n^4+2n^2-1}{2} \rceil} & a_1^{\lceil \frac{2n^4+2n^2-1}{2} \rceil + 1} & \dots & a_1^{2n^4+2n^2-2} \\ \vdots & \vdots & \ddots & \vdots & \vdots & \vdots & \ddots & \vdots \\ 0 & 0 & \dots & 0 & a_{2n^4+2n^2-1}^{\lceil \frac{2n^4+2n^2-1}{2} \rceil} & a_{2n^4+2n^2-1}^{\lceil \frac{2n^4+2n^2-1}{2} \rceil + 1} & \dots & a_{2n^4+2n^2-1}^{2n^4+2n^2-2} \end{bmatrix}, \quad (88)$$

and

$$D = \begin{bmatrix} \text{diag}(u) & 0 \\ 0 & \text{diag}(v) \end{bmatrix}. \quad (89)$$

### 5.2.2 $K = L = n^k$ and $T = n^m$

The following are the exponents, and the corresponding degree table is given in Table 2,

$$\alpha_1 = \beta_1 = [0, 1, \dots, n^m - 1], \quad (90)$$

$$\alpha_2 = [n^m + n^{2k} - n^k, n^m + n^{2k} - n^k + 1, \dots, n^m + n^{2k} - 1], \quad (91)$$

$$\beta_2 = [2n^m - 1, 2n^m + n^k - 1, \dots, 2n^m + n^{2k} - n^k - 1]. \quad (92)$$

The encoding is done as follows,

$$f(x) = \sum_{i=1}^{n^m} R_i x^{\alpha(i)} + \sum_{i=1}^{n^k} A_i x^{\alpha(i+n^m)}, \quad (93)$$

$$g(x) = \sum_{i=1}^{n^m} Z_i x^{\beta(i)} + \sum_{i=1}^{n^k} B_i x^{\beta(i+n^m)}. \quad (94)$$

$\alpha \backslash \beta$	0	1	$\dots$	$n^m - 1$	$2n^m - 1$	$2n^m + n^k - 1$	$\dots$	$2n^m + n^{2k} - n^k - 1$
0	0	$\dots$	$\dots$	$n^m - 1$	$2n^m - 1$	$\dots$	$\dots$	$2n^m + n^{2k} - n^k - 1$
$\vdots$	$\vdots$	$\vdots$	$\ddots$	$\vdots$	$\vdots$	$\vdots$	$\ddots$	$\vdots$
$n^m - 1$	$n^m - 1$	$\dots$	$\dots$	$2n^m - 2$	$3n^m - 2$	$\dots$	$\dots$	$3n^m + n^{2k} - n^k - 2$
$n^m + n^{2k} - n^k$	$n^m + n^{2k} - n^k$	$\dots$	$\dots$	$2n^m + n^{2k} - n^k - 1$	$3n^m + n^{2k} - n^k - 1$	$\dots$	$\dots$	$3n^m + 2n^{2k} - 2n^k - 1$
$\vdots$	$\vdots$	$\vdots$	$\ddots$	$\vdots$	$\vdots$	$\vdots$	$\ddots$	$\vdots$
$n^m + n^{2k} - 1$	$n^m + n^{2k} - 1$	$\dots$	$\dots$	$2n^m + n^{2k} - 2$	$3n^m + n^{2k} - 2$	$\dots$	$\dots$	$3n^m + 2n^{2k} - n^k - 2$

Table 2: Degree table for  $K = L = n^k$ , and  $T = n^m$ .

### 5.2.3 $K = L = n^k$ and $T = n^k + r$

The following are the exponents, and the corresponding degree table is given in Table 3,

$$\alpha_1 = \beta_1 = [0, 1, \dots, n^k + r - 1], \quad (95)$$

$$\alpha_2 = [n^{2k}, n^{2k} + 1, \dots, n^{2k} + n^k - 1], \quad (96)$$

$$\beta_2 = [2n^k + 2r - 1, 3n^k + 2r - 1, \dots, n^{2k} + n^k + 2r - 1]. \quad (97)$$

$\alpha \backslash \beta$	0	1	$\dots$	$n^k + r - 1$	$2n^k + 2r - 1$	$3n^k + 2r - 1$	$\dots$	$n^{2k} + n^k + 2r - 1$
0	0	$\dots$	$\dots$	$n^k + r - 1$	$2n^k + 2r - 1$	$\dots$	$\dots$	$n^{2k} + n^k + 2r - 1$
$\vdots$	$\vdots$	$\vdots$	$\ddots$	$\vdots$	$\vdots$	$\vdots$	$\ddots$	$\vdots$
$n^k + r - 1$	$n^k + r - 1$	$\dots$	$\dots$	$2n^k + 2r - 2$	$3n^k + 3r - 2$	$\dots$	$\dots$	$n^{2k} + 2n^k + 2r - 2$
$n^{2k}$	$n^{2k}$	$\dots$	$\dots$	$n^{2k} + n^k + r - 1$	$n^{2k} + 2n^k + 2r - 1$	$\dots$	$\dots$	$2n^{2k} + n^k + 2r - 1$
$\vdots$	$\vdots$	$\vdots$	$\ddots$	$\vdots$	$\vdots$	$\vdots$	$\ddots$	$\vdots$
$n^{2k} + n^k - 1$	$n^{2k} + n^k - 1$	$\dots$	$\dots$	$n^{2k} + 2n^k + r - 2$	$n^{2k} + 3n^k + 2r - 1$	$\dots$	$\dots$	$2n^{2k} + 2n^k + 2r - 2$

Table 3: Degree table for  $K = L = n^k$ , and  $T = n^m$ .

The encoding is done as follows,

$$f(x) = \sum_{i=1}^T R_i x^{\alpha(i)} + \sum_{i=1}^K A_i x^{\alpha(i+T)}, \quad (98)$$

$$g(x) = \sum_{i=1}^T Z_i x^{\beta(i)} + \sum_{i=1}^L B_i x^{\beta(i+T)}. \quad (99)$$

### 5.2.4 $K \geq L$ and $L = T$

The following are the exponents and the corresponding degree table is given in Table 4,

$$\alpha_1 = \beta_1 = [0, 1, \dots, T-1], \quad (100)$$

$$\alpha_2 = [2T-1, 3T-1, \dots, KT+T-1], \quad (101)$$

$$\beta_2 = [KT, KT+1, \dots, KT+T-1]. \quad (102)$$

$\alpha \backslash \beta$	0	1	$\dots$	$T-1$	$KT$	$KT+1$	$\dots$	$KT+T-1$
0	0	$\dots$	$\dots$	$T-1$	$KT$	$\dots$	$\dots$	$KT+T-1$
$\vdots$	$\vdots$	$\vdots$	$\ddots$	$\vdots$	$\vdots$	$\vdots$	$\ddots$	$\vdots$
$T-1$	$T-1$	$\dots$	$\dots$	$2T-2$	$KT+T-1$	$\dots$	$\dots$	$KT+2T-2$
$2T-1$	$2T-1$	$\dots$	$\dots$	$3T-2$	$KT+2T-1$	$\dots$	$\dots$	$KT+3T-2$
$\vdots$	$\vdots$	$\vdots$	$\ddots$	$\vdots$	$\vdots$	$\vdots$	$\ddots$	$\vdots$
$KT+T-1$	$KT+T-1$	$\dots$	$\dots$	$KT+2T-2$	$2KT+T-1$	$\dots$	$\dots$	$2KT+2T-2$

Table 4: Degree table for  $K \geq L = T$ .

The encoding is done as follows

$$f(x) = \sum_{i=1}^T R_i x^{\alpha(i)} + \sum_{i=1}^K A_i x^{\alpha(T+i)}, \quad (103)$$

$$g(x) = \sum_{i=1}^T Z_i x^{\beta(i)} + \sum_{i=1}^T B_i x^{\beta(T+i)}. \quad (104)$$

### 5.2.5 $K = T = n^k$ and $L = n^\ell$

The following are the exponents, and the corresponding degree table is given in Table 5,

$$\alpha_1 = \beta_1 = [0, 1, \dots, n^k - 1], \quad (105)$$

$$\alpha_2 = [n^{\ell+k}, n^{\ell+k} + 1, \dots, n^{\ell+k} + n^k - 1], \quad (106)$$

$$\beta_2 = [2n^k - 1, 3n^k - 1, \dots, n^{k+\ell} + n^k - 1]. \quad (107)$$

The encoding is done as follows,

$$f(x) = \sum_{i=1}^T R_i x^{\alpha(i)} + \sum_{i=1}^K A_i x^{\alpha(T+i)}, \quad (108)$$

$\alpha \backslash \beta$	0	1	$\dots$	$n^k - 1$	$2n^k - 1$	$3n^k - 1$	$\dots$	$n^{k+\ell} + n^k - 1$
0	0	$\dots$	$\dots$	$n^k - 1$	$2n^k - 1$	$\dots$	$\dots$	$n^{k+\ell} + n^k - 1$
$\vdots$	$\vdots$	$\vdots$	$\dots$	$\vdots$	$\vdots$	$\vdots$	$\dots$	$\vdots$
$n^k - 1$	$n^k - 1$	$\dots$	$\dots$	$2n^k - 2$	$3n^k - 2$	$\dots$	$\dots$	$n^{k+\ell} + 2n^k - 2$
$n^{k+\ell}$	$n^{k+\ell}$	$\dots$	$\dots$	$n^{k+\ell} + n^k - 1$	$n^{k+\ell} + 2n^k - 1$	$\dots$	$\dots$	$2n^{k+\ell} + n^k - 1$
$\vdots$	$\vdots$	$\vdots$	$\dots$	$\vdots$	$\vdots$	$\vdots$	$\dots$	$\vdots$
$n^{k+\ell} + n^k - 1$	$n^{k+\ell} + n^k - 1$	$\dots$	$\dots$	$n^{k+\ell} + 2n^k - 2$	$n^{k+\ell} + 3n^k - 2$	$\dots$	$\dots$	$2n^{k+\ell} + 2n^k - 2$

Table 5: Degree table for  $K = T = n^k$  and  $L = n^\ell$ .

$$g(x) = \sum_{i=1}^T Z_i x^{\beta(i)} + \sum_{i=1}^L B_i x^{\beta(i+T)}. \quad (109)$$

### 5.2.6 $K = T = n^\ell + r$ and $L = n^\ell$

The following are the exponents, and the corresponding degree table is given in Table 6.

$$\alpha_1 = \beta_1 = [0, 1, \dots, n^\ell + r - 1], \quad (110)$$

$$\alpha_2 = [2n^\ell + r - 1, 3n^\ell + r - 1, \dots, n^{2\ell} + (r+1)n^\ell + r - 1], \quad (111)$$

$$\beta_2 = [n^{2\ell} + rn^\ell + r, n^{2\ell} + rn^\ell + r + 1, \dots, n^{2\ell} + (r+1)n^\ell + r - 1]. \quad (112)$$

$\alpha \backslash \beta$	0	1	$\dots$	$n^\ell + r - 1$	$n^{2\ell} + rn^\ell + r$	$n^{2\ell} + rn^\ell + r + 1$	$\dots$	$n^{2\ell} + (r+1)n^\ell + r - 1$
0	0	$\dots$	$\dots$	$n^\ell + r - 1$	$n^{2\ell} + rn^\ell + r$	$\dots$	$\dots$	$n^{2\ell} + (r+1)n^\ell + r - 1$
$\vdots$	$\vdots$	$\vdots$	$\dots$	$\vdots$	$\vdots$	$\vdots$	$\dots$	$\vdots$
$n^\ell + r - 1$	$n^\ell + r - 1$	$\dots$	$\dots$	$2n^\ell + 2r - 2$	$n^{2\ell} + (r+1)n^\ell + 2r - 1$	$\dots$	$\dots$	$n^{2\ell} + (r+2)n^\ell + 2r - 2$
$2n^\ell + r - 1$	$2n^\ell + r - 1$	$\dots$	$\dots$	$3n^\ell + 2r - 2$	$n^{2\ell} + (r+2)n^\ell + 2r - 1$	$\dots$	$\dots$	$n^{2\ell} + (r+3)n^\ell + 2r - 2$
$\vdots$	$\vdots$	$\vdots$	$\dots$	$\vdots$	$\vdots$	$\vdots$	$\dots$	$\vdots$
$n^{2\ell} + (r+1)n^\ell + r - 1$	$n^{2\ell} + (r+1)n^\ell + r - 1$	$\dots$	$\dots$	$n^{2\ell} + (r+2)n^\ell + 2r - 2$	$2n^{2\ell} + (2r+1)n^\ell + 2r - 1$	$\dots$	$\dots$	$2n^{2\ell} + (2r+2)n^\ell + 2r - 2$

Table 6: Degree table for  $K = T = n^\ell + r$ , and  $L = n^\ell$ .

The encoding is done as follows,

$$f(x) = \sum_{i=1}^T R_i x^{\alpha(i)} + \sum_{i=1}^K A_i x^{\alpha(T+i)}, \quad (113)$$

$$g(x) = \sum_{i=1}^T Z_i x^{\beta(i)} + \sum_{i=1}^L B_i x^{\beta(i+T)}. \quad (114)$$

### 5.3 Discussion and Further Remarks

The encoding structure done in this section is different from the previous section where we tried to expand the classical GASP code to the quantum version. In this section, the encoding of the matrix sub-blocks is done over the high-degree terms of the polynomials. There might remain potential for refinement, although it is very difficult to see how, especially since some of them achieve super-dense coding gains in some cases. This extension can happen with more sophisticated dual code tricks that might relax the requirement of (36).

In addition, we noticed, in some cases, even when (36) is not satisfied by GASP, our code has the same number of servers that GASP needs, thus achieving super-dense coding gain as in the case with  $K = T = 8$  and  $L = 2$ .

Finally, it is important to note that when GASP is asymptotically optimal, like the case when  $K = L = T = n^2$ , the asymptotic ratio between the classical and quantum schemes is 1 due to the Holevo bound. To state the bound simply, in a classical-quantum setting, where the entangled transmitters (in our setting,  $N$  entangled transmitters) have classical information to encode over quantum states,  $N$  bits of information can be received by the receiver. Consequently, as  $n \rightarrow \infty$ , we have  $KL \rightarrow N$  as shown in Theorem 14. Thus, the highest possible asymptotic quantum rate is also 1 for entangled transmitters in the quantum PDMM setting.

## 6 PDMM Codes for Low Privacy Regimes

Prior to delving into a newly discovered PDMM codes, the following definition, adopted from [31], is going to be useful for most of the defined codes.

**Definition 10** *Let  $\text{gap}(\ell, x, r) \in \mathbb{Z}^\ell$  be the generalized progression of length  $\ell$  and chain length  $r$ , such that*

$$\begin{aligned} \text{gap}(\ell, x, r) = [ & 0, 1, 2, \dots, r-1, \\ & x, x+1, x+2, \dots, x+r-1, \\ & 2x, 2x+1, 2x+2, \dots, 2x+r-1, \dots ]. \end{aligned} \quad (115)$$

The next three coding schemes only provide better rates than the  $\text{GASP}_r$  when  $T \leq K$ , except for optimized GASP, which consistently does not perform worse than GASP. However, it is challenging to come up with situations where they provide better rates and can satisfy (36). This is mainly because, in order to provide more efficiency to the schemes, more gaps in the exponents are added to decrease the number of servers. However, in one case for the  $\text{CAT}_x$  code, we are able to satisfy the required constraint (36) when  $T = K = L = 2$ , and have better efficiency than GASP. This shows that there can exist cases for these three codes that can be extended to their quantum version, and at the same time, have better efficiency



than the  $\text{GASP}_r$  code.

To that end, we rewrite the construction of the three aforementioned codes and design the quantum  $\text{CAT}_x$  code for the special case of  $K = L = T = 2$ . We note again that these codes can possibly be extended to the quantum case if (36) is satisfied.

**Definition 11 (Optimized GASP ( $\text{GASP}_{r,s}$ ) codes)** *Given  $K, L$  and  $T \geq 2$ , let  $1 \leq r, s \leq \min(K, T)$ . Then, the  $\text{GASP}_{r,s}$  exponents are given by*

$$\alpha_1 = [0 : K - 1], \quad (116)$$

$$\alpha_2 = KL + \text{gap}(T, K, r), \quad (117)$$

$$\beta_1 = K \times [0 : L - 1], \quad (118)$$

$$\beta_2 = KL + \text{gap}(T, K, s). \quad (119)$$

**Definition 12 ( $\text{DOG}_{r,s}$  codes)** *Given  $K, L$  and  $T \geq 2$ , let  $1 \leq r \leq T$  and  $1 \leq s \leq \min(K + r, T)$ . Then, the  $\text{DOG}_{r,s}$  exponents are given by,*

$$\alpha_1 = [0 : K - 1], \quad (120)$$

$$\alpha_2 = K + \text{gap}(T, K + r, r), \quad (121)$$

$$\beta_1 = (K + r) \times [0 : L - 1], \quad (122)$$

$$\beta_2 = (K + r)(L - 1) + K + \text{gap}(T, K + r, s). \quad (123)$$

**Definition 13 ( $\text{CAT}_x$  codes)** *For  $K \geq L \geq T \geq 2$ , let  $\kappa$  and  $\lambda$  be the smallest non-negative integers that make  $K^* = K + 1 + \kappa$  and  $L^* = L + 1 + \lambda$  be co-primes with  $\bar{T} = T - 1$ . Let  $q = K^*L^* + \bar{T}^2$ , and  $x$  be any number co-prime with  $q$ . Finally, let  $y$  be the solution to  $x\bar{T} + yK^* = 0 \pmod{q}$ . Then, the exponents of  $\text{CAT}_x(K, L, T)$  are given by*

$$\alpha_1 = y \times [0 : K - 1] \pmod{q}, \quad (124)$$

$$\alpha_2 = x \times [0 : T - 1] + Ky \pmod{q}, \quad (125)$$

$$\beta_1 = x \times [0 : L - 1] \pmod{q}, \quad (126)$$

$$\beta_2 = y \times [0 : T - 1] - x \pmod{q}. \quad (127)$$

## 6.1 Schrödinger $\text{CAT}_x(2, 2, 2)$ Code

Instead of calling it the quantum CAT code, we choose that name for obvious reasons. In this section, we extend the classical  $\text{CAT}_x(2, 2, 2)$  to the quantum version since this is the only code with these specific parameters that we are able to find that provides a better rate than  $\text{GASP}_r$  and at the same time satisfies (36).

Prior to delving into the quantum encoding, we refer the reader to the classical construction of this specific example in [31]. To summarize,  $N = q = 10$ , the root of unity chosen is 2

and  $\omega_i = 2^{i-1}$ . Thus, the generator matrix can be written as  $[n, n, d]_{11}$   $\text{GRS}(\omega, u) = \text{GRS}_{\omega, u}$ , where  $u = [1, 1, \dots, 1]$ . We can write the classical transmitted symbols as,

$$Y(i, j) = \text{GRS}_{\omega, u} \left[ A_1 B_1(i, j), A_1 B_2(i, j), I_1(i, j), A_2 B_1(i, j), A_2 B_2(i, j), \right. \\ \left. I_2(i, j), I_3(i, j), I_4(i, j), I_5(i, j), I_6(i, j) \right]^t \quad (128)$$

$$= \begin{bmatrix} G_1 & H_1 \end{bmatrix} \begin{bmatrix} I_2(i, j), I_3(i, j), I_4(i, j), I_5(i, j), I_6(i, j), \\ A_1 B_1(i, j), A_1 B_2(i, j), I_1(i, j), A_2 B_1(i, j), A_2 B_2(i, j) \end{bmatrix}^t, \quad (129)$$

where  $G_1 = \text{GRS}_{\omega, u}(:, 6 : 10)$  and  $H_1 = \text{GRS}_{\omega, u}(:, 1 : 5)$ .

It is straightforward to verify that  $G_1$  can be considered as  $[10, 5, d_1]_{11}$  5-shifted GRS code. The 5-shifted  $[10, 5, d_2]_{11}$  dual code can be generated by  $\omega$  and  $v$ , where  $v$  satisfies (6) with  $\ell_1 = \ell_2 = 5$ . Let the generator matrix of the dual code be defined as  $G_2$ , and it can be verified that  $\begin{bmatrix} G_1 & 0 \\ 0 & G_2 \end{bmatrix}$  is an SSO matrix. In addition, we choose  $H_2 = \text{GRS}_{\omega, v}(:, 1 : 5)$ . The received symbols from the quantum scheme can be written as,

$$Y(i, j) = \begin{bmatrix} 0 & I \end{bmatrix} \begin{bmatrix} G_1 & 0 & H_1 & 0 \\ 0 & G_2 & 0 & H_2 \end{bmatrix}^{-1} \begin{bmatrix} G_1 & 0 & H_1 & 0 \\ 0 & G_2 & 0 & H_2 \end{bmatrix} \\ \times \begin{bmatrix} I_2^{[1]}(i, j), I_3^{[1]}(i, j), I_4^{[1]}(i, j), I_5^{[1]}(i, j), I_6^{[1]}(i, j), \\ I_2^{[2]}(i, j), I_3^{[2]}(i, j), I_4^{[2]}(i, j), I_5^{[2]}(i, j), I_6^{[2]}(i, j), \\ A_1 B_1^{[1]}(i, j), A_1 B_2^{[1]}(i, j), I_1^{[1]}(i, j), A_2 B_1^{[1]}(i, j), A_2 B_2^{[1]}(i, j) \\ A_1 B_1^{[2]}(i, j), A_1 B_2^{[2]}(i, j), I_1^{[2]}(i, j), A_2 B_1^{[2]}(i, j), A_2 B_2^{[2]}(i, j) \end{bmatrix}^t \quad (130)$$

$$= \begin{bmatrix} A_1 B_1^{[1]}(i, j), A_1 B_2^{[1]}(i, j), I_1^{[1]}(i, j), A_2 B_1^{[1]}(i, j), A_2 B_2^{[1]}(i, j) \\ A_1 B_1^{[2]}(i, j), A_1 B_2^{[2]}(i, j), I_1^{[2]}(i, j), A_2 B_1^{[2]}(i, j), A_2 B_2^{[2]}(i, j) \end{bmatrix}^t. \quad (131)$$

Thus, we are able to achieve a quantum rate that is double the highest classical state-of-the-art version, i.e.,  $R_Q = 4/5$ .

## 6.2 Discussion and Further Remarks

Although we are not able to find many situations where the optimal code out of the three codes, optimized GASP, CAT and DOG, satisfy the feasibility constraint in (36) and at the same time have better performance than GASP, here we presented a simple example that shows that it indeed can happen. This makes the search for a relaxed version of the feasibility requirement an urgent matter so that these codes can be extended to their quantum counterparts.

## 7 A Family of Codes for PDMM in the Low Privacy Regime

Although many regimes are covered in the previous sections, the case where  $T < \min(K, L) = L$  is still the main missing piece in our work. An interesting approach to look at is to increase the security parameters to one of the polynomials, i.e., instead of

$$g(x) = \sum_{i=1}^L B_i x^{\beta(i)} + \sum_{j=1}^T R_j x^{\beta(j+L)}, \quad (132)$$

we can extend this to  $\bar{T} > T$ , such that

$$g(x) = \sum_{i=1}^L B_i x^{\beta(i)} + \sum_{j=1}^{\bar{T}} R_j x^{\beta(j+L)}. \quad (133)$$

The  $\bar{T}$  is added in a way that makes the transfer matrix extendable to the quantum version. As a starting example, let  $K = L = 2$  and  $T = 1$ . The GASP exponents are given by

$$\alpha = [0, 2, 4], \quad \beta = [0, 1, 4]. \quad (134)$$

The rate in this case is given by  $R_C = \frac{1}{2}$ . Unfortunately, this is not directly extendable to the quantum version. However, if we change the code to the following exponents

$$\alpha = [0, 2, 4], \quad \beta = [0, 1, 4, 5], \quad (135)$$

then this can be extended to the quantum version, and the rate is given by  $R_Q = \frac{4}{5}$ .

Another example is when  $K = L = 3$  and  $T = 1$ . In this case, we have the following exponents for the GASP

$$\alpha = [0, 1, 2, 9], \quad \beta = [0, 3, 6, 9], \quad (136)$$

with the information encoded over the first three elements of each exponent vector,  $\alpha$  and  $\beta$ . The rate in this case is  $R_C = \frac{9}{15}$ . However, this is very hard to change directly with the information sub-space being the same like the previous example. If we choose  $\bar{T} = 3$ , we can design the following exponents

$$\alpha = [0, 3, 5, 7], \quad \beta = [0, 1, 2, 10, 18, 26], \quad (137)$$

achieving a rate equal to  $R_Q = \frac{18}{22} = \frac{9}{11}$ . Thus, the approach that we take is to use  $\bar{T}$  instead of  $T$  in one of the polynomials and encode the useful information over the higher degree part of the resulting polynomial.

## 7.1 Main Results

**Theorem 15** *Let  $K \geq L \geq T$ , with  $2mL \geq \delta L + (m-2)(T-1) + (m-1)L^2 + 6$ . Then, there exists a quantum code that is based on a polynomial code that satisfies the PDMM requirements, achieving a rate equal to*

$$R_Q = \frac{2KL}{K(L+3) + (m+2)(T-1) + L^2 - 2L}, \quad (138)$$

where  $K = m(L-1) + \delta$  and  $0 \leq \delta < L-1$ .

**Corollary 7** *If  $K = L > T$  with  $L+T \geq 7$ , then there exists a quantum code that is based on a polynomial code that satisfies the PDMM requirements, achieving a rate equal to*

$$R_Q = \frac{2L^2}{2L^2 + L + 3T - 3}. \quad (139)$$

To understand the ratio between the highest classical rate and our achieved rate in the low privacy regime, Figs. 10-13 are shown for numerical representation for the  $K = L > T$  case since this case is less complicated. The figures suggests two things, the first is that when  $T$  is small, the code designed is not going to be as efficient as in the high privacy regimes. This is mainly because the interference subspace, i.e., the subspace that carries no information about the multiplication  $AB$ , is small compared to the whole space, which makes it harder to optimize since fewer terms can be dropped. The second reason is that the classical codes are efficient so that the rate is close enough to the unity which makes the quantum codes not being able to surpass the classical counterparts by much due to the Holevo bound.

## 7.2 Encoding Structure

To make it easier to visualize, we first start by proving Corollary 7, and then go the more general setting. The construction of the  $G$  and  $H$  matrices follows similar to Section 5.2.

### 7.2.1 $K = L > T$

The following are the exponents, and the corresponding degree table is given in Table 7,

$$\alpha_1 = [0 : L-1], \quad (140)$$

$$\beta_1 = [0 : T-1], \quad (141)$$

$$\alpha_2 = [\underbrace{L^2 + T - 1, L^2 + T, \dots, L^2 + L + T - 3}_{L-1}, 2L^2 + 2T - 3], \quad (142)$$

$$\beta_2 = [T + L - 2, T + 2L - 3, \dots, L^2 - L + T - 1]. \quad (143)$$

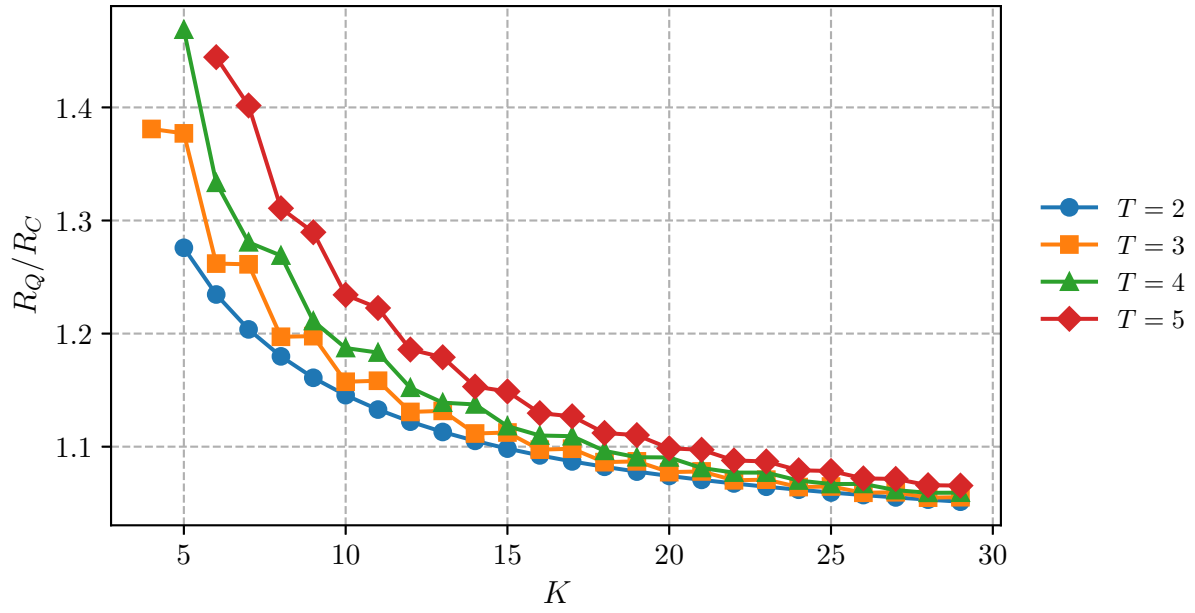


Figure 10:  $K = L$  and  $T = [2 : 5]$ .

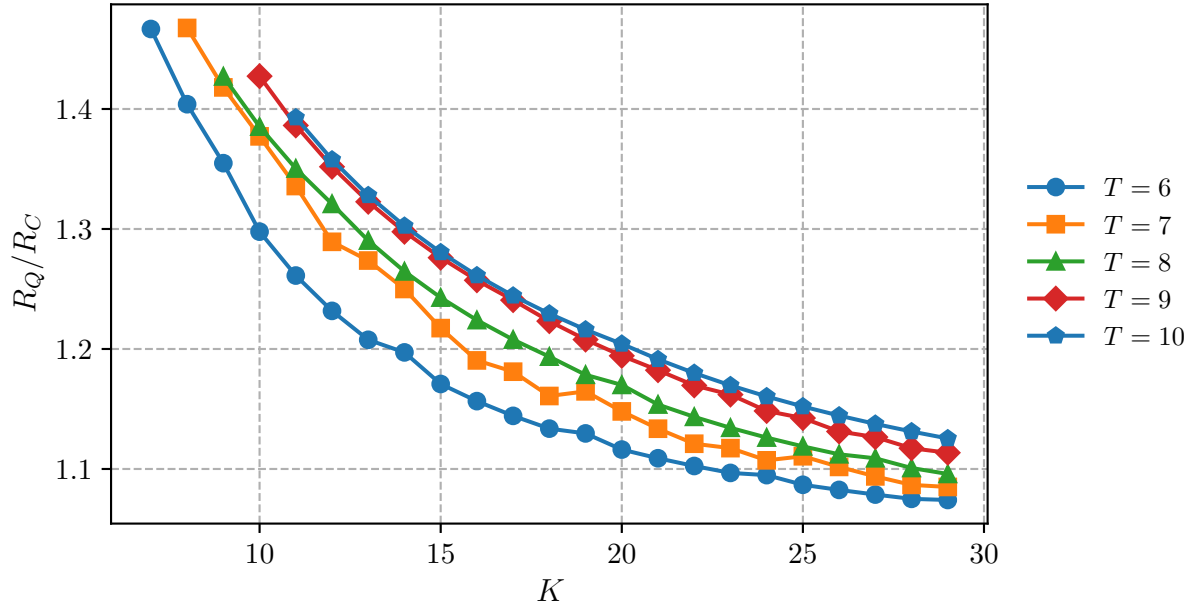


Figure 11:  $K = L$  and  $T = [6 : 10]$ .

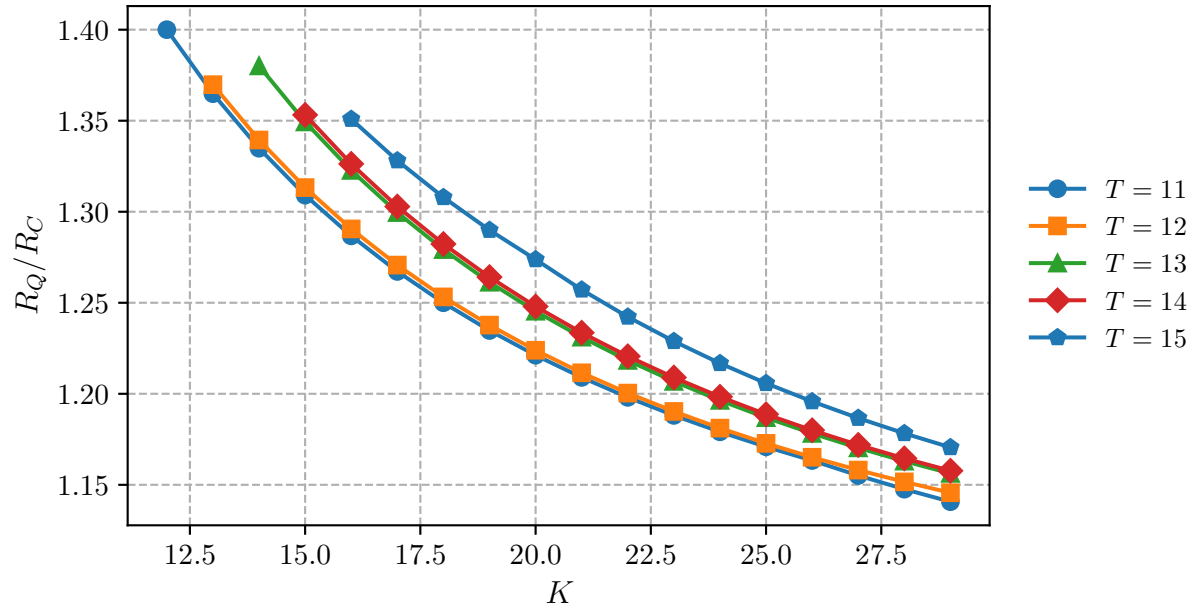


Figure 12:  $K = L$  and  $T = [11 : 15]$ .

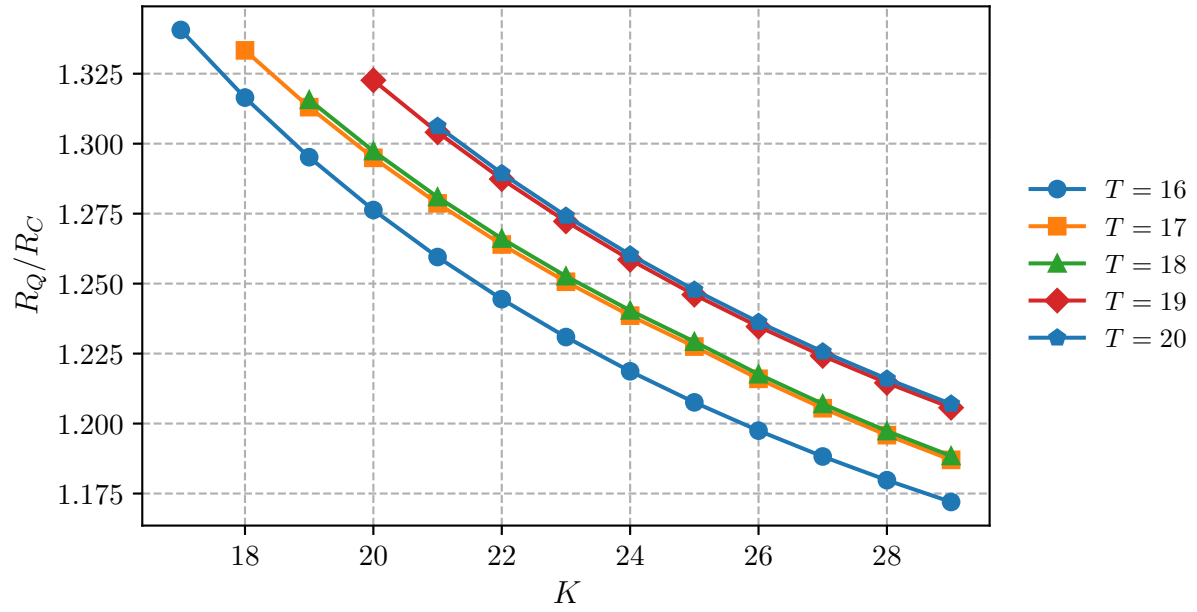


Figure 13:  $K = L$  and  $T = [16 : 20]$ .

$\alpha \backslash \beta$	0	1	$\dots$	$T-1$	$T+L-2$	$T+2L-3$	$\dots$	$L^2-L+T-1$
0	0	$\dots$	$\dots$	$T-1$	$T+L-2$	$\dots$	$\dots$	$L^2-L+T-1$
1	$\vdots$	$\ddots$	$\ddots$	$\vdots$	$\vdots$	$\ddots$	$\ddots$	$\vdots$
$\vdots$	$\vdots$	$\vdots$	$\dots$	$\vdots$	$\vdots$	$\vdots$	$\dots$	$\vdots$
$L-1$	$L-1$	$\dots$	$\dots$	$T+L-2$	$T+2L-3$	$\dots$	$\dots$	$L^2+T-2$
$L^2+T-1$	$L^2+T-1$	$\dots$	$\dots$	$L^2+2T-2$	$L^2+L+2T-3$	$\dots$	$\dots$	$2L^2-L+2T-2$
$\vdots$	$\vdots$	$\vdots$	$\dots$	$\vdots$	$\vdots$	$\vdots$	$\dots$	$\vdots$
$L^2+L+T-3$	$L^2+L+T-3$	$\dots$	$\dots$	$L^2+L+2T-4$	$L^2+2L+2T-5$	$\dots$	$\dots$	$2L^2+2T-4$
$2L^2+2T-3$	$2L^2+2T-3$	$\dots$	$\dots$	$2L^2+3T-4$	$2L^2+3T+L-5$	$2L^2+3T+2L-6$	$\dots$	$3L^2-L+3T-4$

Table 7: Degree table for  $K = L > T$ .

The encoding is done as follows,

$$f(x) = \sum_{i=1}^L R_i x^{\alpha(i)} + \sum_{j=1}^L A_j x^{\alpha(T+j)}, \quad (144)$$

$$g(x) = \sum_{i=1}^T Z_i x^{\beta(i)} + \sum_{j=1}^L B_j x^{\beta(T+j)}. \quad (145)$$

To show that the code is a valid quantum PDMM code, since there are gaps in the last row, we check a slight variation of the feasibility condition in (36). We check the longest chain of consecutive exponents in the degree table for the interference subspace, i.e., the part of the degree Table 7 excluding  $\alpha_2 \oplus \beta_2$ . Thus, the longest chain is  $[0 : L^2 + L + 2T - 4]$ . To that end, we need to make sure that it is greater than the ceiling of half of the number of servers, i.e.,  $L^2 + L + 2T - 4 \geq \lceil \frac{2L^2+L+3T-3}{2} \rceil$ . To proceed, we need to prove that  $L^2 + L + 2T - 4 \geq \lceil \frac{2L^2+L+3T-3}{2} \rceil$ . Recall that  $L + T \geq 7$ , then we have

$$\frac{L+T}{2} \geq 3.5 \Rightarrow L^2 + L + 2T - 4 \geq L^2 + \frac{L}{2} + 1.5T - 0.5 \quad (146)$$

$$\Rightarrow L^2 + L + 2T - 4 \geq \frac{2L^2 + L + 3T - 3}{2} + 1 \quad (147)$$

$$\Rightarrow L^2 + L + 2T - 4 \geq \left\lceil \frac{2L^2 + L + 3T - 3}{2} \right\rceil. \quad (148)$$

## 7.2.2 $K \geq L > T$

First, assume that  $K = m(L-1) + \delta$ ,  $0 \leq \delta < L-1$ . Then, the following are the exponents and the corresponding degree table is given in Table 8,

$$\alpha_1 = [0 : K-1], \quad (149)$$

$$\beta_1 = [0 : T-1], \quad (150)$$

$$\alpha'_1 = \underbrace{[2K + T + L^2 - 2L - 1, 2K + T + L^2 - 2L, \dots, 2K + T + L^2 - L - 3]}_{L-1}, \quad (151)$$

$$\alpha'_2 = \underbrace{[3K + 2T + 2L^2 - 2L - 3, 3K + 2T + 2L^2 - 2L - 2, \dots, 3K + 2T + 2L^2 - 2L - 5]}_{L-1}, \quad (152)$$

$\vdots$

$$\alpha'_m = [(m+1)K + mT + mL^2 - (m+1)L - 2m + 1, (m+1)K + mT + mL^2 - (m+1)L - 2m + 2, \dots, (m+1)K + mT + mL^2 - mL - 2m - 1], \quad (153)$$

$$\alpha'' = [(m+2)K + (m+1)T + (m+1)L^2 - (m+2)L - 2m - 1, (m+2)K + (m+1)T + (m+1)L^2 - (m+2)L - 2m, \dots, (m+2)K + (m+1)T + (m+1)L^2 - (m+2)L - 2m + \delta - 2] \quad (154)$$

$$\beta_2 = [K + T - 2, K + T + L - 3, \dots, K + T + L^2 - 2L - 1], \quad (155)$$

where  $\alpha_2 = [\alpha'_1, \dots, \alpha'_m, \alpha'']$ , with each  $\alpha'_i$ ,  $i \in [m]$  is of length  $L - 1$ , and  $\alpha''$  is of length  $\delta$ .

The encoding is done as follows

$$f(x) = \sum_{i=1}^K R_i x^{\alpha(i)} + \sum_{j=1}^K A_j x^{\alpha(K+j)}, \quad (156)$$

$$g(x) = \sum_{i=1}^T Z_i x^{\beta(i)} + \sum_{j=1}^L B_j x^{\beta(T+j)}. \quad (157)$$

### 7.3 Discussion and Further Remarks

In this section, we proposed a method to address the low privacy regime case, where  $T$  is small compared to  $K$  and  $L$ . There might be room for refinement in this case, as suggested by observations in the classical setting, where different codes compete for efficiency in this regime with no single scheme demonstrating consistent superiority. We proposed extending only one polynomial with an extra privacy requirement so that it becomes extendable to the quantum version. As shown in the figures presented in this section, the gain is at most 1.5. This suggests that more efficient code constructions may exist.

An alternative approach to address this problem is to distribute the privacy to both polynomials equally until (36) is satisfied for one of the classical codes and then use it in that new setting with extra privacy constraint. Preliminary evaluations indicate that this approach might be less efficient than the proposed one in this section.

Finally, a particularly promising yet challenging direction is the entanglement-assisted framework, reformulated recently in [46], where local precoding matrix is used at each server. The main obstacle is to find the precoding that can enhance the achievable rate.



$\alpha \backslash \beta$	0	1	$\dots$	$T-1$	$K+T-2$	$K+T+L-3$	$\dots$	$K+T+L^2-2L-1$
0	0	$\dots$	$\dots$	$T-1$	$K+T-2$	$\dots$	$\dots$	$K+T+L^2-2L-1$
1	$\vdots$	$\ddots$	$\ddots$	$\vdots$	$\vdots$	$\ddots$	$\ddots$	$\vdots$
$\vdots$	$\vdots$	$\vdots$	$\dots$	$\vdots$	$\vdots$	$\vdots$	$\dots$	$\vdots$
$K-1$	$K-1$	$\dots$	$\dots$	$K+T-2$	$2K+T-3$	$\dots$	$\dots$	$2K+T+L^2-2L-2$
$2K+T+L^2-2L-1$	$2K+T+L^2-2L-1$	$\dots$	$\dots$	$2K+2T+L^2-2L-2$	$3K+2T+L^2-2L-3$	$\dots$	$\dots$	$3K+2T+2L^2-4L-2$
$\vdots$	$\vdots$	$\vdots$	$\dots$	$\vdots$	$\vdots$	$\vdots$	$\dots$	$\vdots$
$2K+T+L^2-L-3$	$2K+T+L^2-L-3$	$\dots$	$\dots$	$2K+2T+L^2-L-4$	$3K+2T+L^2-L-5$	$\dots$	$\dots$	$3K+2T+2L^2-3L-4$
$3K+2T+2L^2-2L-3$	$3K+2T+2L^2-2L-3$	$\dots$	$\dots$	$3K+3T+2L^2-2L-4$	$4K+3T+2L^2-2L-5$	$\dots$	$\dots$	$4K+3T+3L^2-4L-4$
$\vdots$	$\vdots$	$\vdots$	$\dots$	$\vdots$	$\vdots$	$\vdots$	$\dots$	$\vdots$
$3K+2T+2L^2-L-5$	$3K+2T+2L^2-L-5$	$\dots$	$\dots$	$3K+3T+2L^2-2L-6$	$4K+3T+2L^2-2L-7$	$\dots$	$\dots$	$4K+3T+3L^2-3L-6$
$\vdots$	$\dots$	$\dots$	$\dots$	$\vdots$	$\dots$	$\dots$	$\dots$	$\dots$
$(m+1)K+mT+mL^2-(m+1)L-2m+1$	$(m+1)K+mT+mL^2-(m+1)L-2m+1$	$\dots$	$\dots$	$(m+1)K+(m+1)T+mL^2-(m+1)L-2m$	$(m+2)K+(m+1)T+mL^2-(m+1)L-2m-1$	$\dots$	$\dots$	$(m+2)K+(m+1)T+(m+1)L^2-(m+3)L-2m$
$\vdots$	$\vdots$	$\vdots$	$\dots$	$\vdots$	$\vdots$	$\vdots$	$\dots$	$\vdots$
$(m+1)K+mT+mL^2-mL-2m-1$	$(m+1)K+mT+mL^2-mL-2m-1$	$\dots$	$\dots$	$(m+1)K+(m+1)T+mL^2-mL-2m$	$(m+2)K+(m+1)T+mL^2-mL-2m-3$	$\dots$	$\dots$	$(m+2)K+(m+1)T+(m+1)L^2-(m+2)L-2m-2$
$(m+2)K+(m+1)T+(m+1)L^2-(m+2)L-2m-1$	$(m+2)K+(m+1)T+(m+1)L^2-(m+2)L-2m-1$	$\dots$	$\dots$	$(m+2)K+(m+2)T+(m+1)L^2-(m+2)L-2m-2$	$(m+3)K+(m+2)T+(m+1)L^2-(m+2)L-2m-3$	$\dots$	$\dots$	$(m+3)K+(m+2)T+(m+2)L^2-(m+4)L-2m-1$
$\vdots$	$\vdots$	$\vdots$	$\dots$	$\vdots$	$\vdots$	$\vdots$	$\dots$	$\vdots$
$(m+2)K+(m+1)T+(m+1)L^2-(m+2)L-2m+\delta-2$	$(m+2)K+(m+1)T+(m+1)L^2-(m+2)L-2m+\delta-2$	$\dots$	$\dots$	$(m+2)K+(m+2)T+(m+1)L^2-(m+2)L-2m+\delta-3$	$(m+3)K+(m+2)T+(m+1)L^2-(m+2)L-2m+\delta-4$	$\dots$	$\dots$	$(m+3)K+(m+2)T+(m+2)L^2-(m+4)L-2m+\delta-3$

Table 8: Degree table for  $K \geq L > T$ .

## 8 Conclusion

In this paper, we investigated the problem of private distributed matrix multiplication (PDMM) for the case of outer product partitioning (OPP) in the quantum setting, i.e., the QPDMM problem. First, we formulated the quantum setting for the PDMM problem when the servers share an entangled state. Second, we divided our approach into two regimes based on the privacy requirement. In the first regime, we extended the state-of-the-art classical coding scheme, i.e., gap additive secure polynomial (GASP) code, when a feasibility condition is satisfied. We showed that when this condition is satisfied, super-dense coding gain is achieved, i.e., the rate of the quantum setting is double its counterpart in the classical setting. We showed this by developing a quantum scheme that can encode two instances

of the GASP code in the quantum setting instead of one instance in the classical setting. Third, we analyzed the case when the feasibility condition is not satisfied. We designed several quantum schemes based on the system parameters in order to compensate for the inapplicability of the feasibility condition. We compared the designed quantum codes and their counterpart of the state-of-the-art classical code in several settings. We showed that super-dense coding gain can still be achieved in some cases. In addition, we observed that the gain plots show that the gain ranges from 2 to 1 in this regime.

Fourth, we investigated the low privacy regime in the same framework. We analyzed how to extend the state-of-the-art classical codes, i.e., the cyclic-addition degree table (CAT) and the discretely optimized GASP (DOG) codes. We gave a specific numerical example when the CAT code can be extended to the quantum setting, achieving the super-dense coding gain. Finally, we directly designed quantum codes for the low privacy regime. The design for these codes is influenced by previous work on the quantum version of the private information retrieval (QPIR) problem by extending the privacy requirement slightly. The plots show that the gain varies from 1.5 to 1 in this regime.

## References

- [1] I. Goodfellow, Y. Bengio, and A. Courville. *Deep Learning*. MIT Press, November 2016.
- [2] A. Vaswani, N. Shazeer, N. Parmar, J. Uszkoreit, L. Jones, A. Gomez, Ł. Kaiser, and I. Polosukhin. Attention is all you need. *NeurIPS*, 30:59986008, December 2017.
- [3] E. Candès, J. Romberg, and T. Tao. Robust uncertainty principles: Exact signal reconstruction from highly incomplete frequency information. *IEEE Trans. Info. Theory*, 52(2):489509, February 2006.
- [4] A. Yao. Protocols for secure computations. In *Annual Symposium on Foundations of Computer Science (FOCS)*, November 1982.
- [5] D. Chaum, I. Damgård, and J. van de Graaf. Multiparty computations ensuring privacy of each party’s input and correctness of the result. In *Advances in Cryptology (CRYPTO)*, August 1988.
- [6] M. Jakobsson and A. Juels. Mix and match: Secure function evaluation via ciphertexts. In *Advances in Cryptology (ASIACRYPT)*, December 2000.
- [7] S. Rane, W. Sun, and A. Vetro. Secure function evaluation based on secret sharing and homomorphic encryption. In *Allerton Conference*, September 2009.
- [8] M. van Dijk, C. Gentry, S. Halevi, and V. Vaikuntanathan. Fully homomorphic encryption over the integers. In *Advances in Cryptology (EUROCRYPT)*, May 2010.

- [9] K. Khan and M. Shaheen. Secure cloud services: Matrix multiplication revisited. In *IEEE CSE*, December 2013.
- [10] W. Chang and R. Tandon. On the capacity of secure distributed matrix multiplication. In *IEEE Globecom*, December 2018.
- [11] Z. Jia and S. Jafar. On the capacity of secure distributed batch matrix multiplication. *IEEE Trans. Info. Theory*, 67(11):74207437, September 2021.
- [12] R. DOliveira, S. Rouayheb, D. Heinlein, and D. Karpuk. Notes on communication and computation in secure distributed matrix multiplication. In *IEEE CNS*, June 2020.
- [13] H. López, G. Matthews, and D. Valvo. Secure matdot codes: a secure, distributed matrix multiplication scheme. In *IEEE ITW*, November 2022.
- [14] R. Machado, G. Matthews, and W. Santos. Hera scheme: Secure distributed matrix multiplication via hermitian codes. In *IEEE ISIT*, June 2023.
- [15] D. Malak. Distributed structured matrix multiplication. In *IEEE ISIT*, June 2024.
- [16] J. Li, O. Makkonen, C. Hollanti, and O. Gnille. Efficient recovery of a shared secret via cooperation: Applications to SDMM and PIR. *IEEE Jour. Sel. Areas Commun.*, 40(3):871884, January 2022.
- [17] R. Machado and F. Manganiello. Root of unity for secure distributed matrix multiplication: Grid partition case. In *IEEE ITW*, November 2022.
- [18] O. Makkonen and C. Hollanti. Analog secure distributed matrix multiplication over complex numbers. In *IEEE ISIT*, June 2022.
- [19] N. Mital, C. Ling, and D. Gündüz. Secure distributed matrix computation with discrete fourier transform. *IEEE Trans. Info. Theory*, 68(7):46664680, March 2022.
- [20] S. Dutta, M. Fahim, F. Haddadpour, H. Jeong, V. Cadambe, and P. Grover. On the optimal recovery threshold of coded matrix multiplication. *IEEE Trans. Info. Theory*, 66(1):278301, July 2020.
- [21] Q. Yu and A. Avestimehr. Entangled polynomial codes for secure, private, and batch distributed matrix multiplication: Breaking the “cubic” barrier. In *IEEE ISIT*, August 2020.
- [22] J. Choi, J. Dongarra, and D. Walker. Scalable matrix multiply on distributed-memory parallel computers. *Jour. of Paral. and Dist. Comp.*, 33(1), February 1996.

- [23] E. Solomonik, D. Matthews, J. R. Hammond, J. F. Stanton, and J. Demmel. Cyclops tensor framework: Reducing communication and eliminating load imbalance in massively parallel contractions. *IEEE IPDPS*, May 2014.
- [24] S. K. Khatamifard, U. Upadhyay, and C. De Sa. Outer-product attention with performance guarantees. *ICML*, July 2023.
- [25] B. Hasrcolu, J. Gómez-Vilardebó, and D. Gündüz. Bivariate polynomial codes for secure distributed matrix multiplication. *IEEE Jour. Sel. Areas Commun.*, 40(3):955967, January 2022.
- [26] J. Gómez-Vilardebó, B. Hasrcolu, and D. Gündüz. Generalized multivariate polynomial codes for distributed matrix-matrix multiplication. In *IEEE ITW*, November 2024.
- [27] R. Cartor, R. D’Oliveira, S. El Rouayheb, D. Heinlein, D. Karpuk, and A. Sprintson. Secure distributed matrix multiplication with precomputation. In *IEEE ISIT*, June 2024.
- [28] O. Makkonen, E. Saçkara, and C. Hollanti. Algebraic geometry codes for secure distributed matrix multiplication. *IEEE Trans. Info. Theory*, 71(4):23732382, January 2025.
- [29] S. Kiani and S. Draper. Successive approximation for coded matrix multiplication. In *IEEE ISIT*, June 2022.
- [30] R. D’Oliveira, S. El Rouayheb, and D. Karpuk. GASP codes for secure distributed matrix multiplication. *IEEE Trans. Info. Theory*, 66(7):40384050, July 2020.
- [31] C. Hofmeister, R. Bitar, and A. Wachter-Zeh. CAT and DOG: Improved codes for private distributed matrix multiplication, 2025. Available online at arXiv:2501.12371.
- [32] C. Bennett and S. Wiesner. Communication via one- and two-particle operators on Einstein-Podolsky-Rosen states. *Physical Review Letters*, 69(20):28812884, November 1992.
- [33] M. Allaix, Y. Lu, Y. Yao, T. Pillaha, C. Hollanti, and S. A. Jafar.  $N$ -sum box: An abstraction for linear computation over many-to-one quantum networks. *IEEE Trans. Info. Theory*, 71(2):1121–1139, December 2025.
- [34] A. Aytekin, M. Nomeir, S. Vithana, and S. Ulukus. Quantum symmetric private information retrieval with secure storage and eavesdroppers. In *IEEE Globecom*, December 2023.

- [35] A. Aytakin, M. Nomeir, S. Vithana, and S. Ulukus. Quantum  $X$ -secure  $E$ -eavesdropped  $T$ -colluding symmetric private information retrieval. *IEEE Trans. Info. Theory*, 71(5):3974–3988, March 2025.
- [36] A. Aytakin, M. Nomeir, and S. Ulukus. Quantum  $X$ -secure  $B$ -Byzantine  $T$ -colluding private information retrieval. 2024. Available online at <http://www.ece.umd.edu/~ulukus/papers/journal/QXBTPIR.pdf>.
- [37] M. Nomeir, A. Aytakin, and S. Ulukus. Quantum  $X$ -secure  $B$ -Byzantine  $T$ -colluding private information retrieval. In *IEEE ITW*, November 2024.
- [38] M. Nomeir, A. Aytakin, and S. Ulukus. Byzantine-eavesdropper alliance: How to achieve symmetric privacy in quantum  $X$ -secure  $B$ -Byzantine  $E$ -eavesdropped  $U$ -unresponsive  $T$ -colluding PIR? *IEEE Transactions on Information Theory*, 2025.
- [39] Y. Lu and S. Jafar. A coding scheme for straggler resilient quantum  $X$ -secure  $T$ -private information retrieval. 2023. Available online at arXiv:2311.07829.
- [40] Y. Lu, Y. Yao, and S. Jafar. On the capacity of secure  $K$ -user product computation over a quantum MAC. *IEEE Comm. Letters*, 27(10):2598–2602, September 2023.
- [41] Y. Yao and S. A. Jafar. The capacity of classical summation over a quantum MAC with arbitrarily distributed inputs and entanglements. *IEEE Trans. Info. Theory*, 70(9):6350–6370, May 2024.
- [42] Y. Yao and S. Jafar. The inverted 3-sum box: General formulation and quantum information theoretic optimality. 2024. Available online at arxiv:2407.01498.
- [43] Jacobus H. van Lint. *Introduction to Coding Theory*, volume 86 of *Graduate Texts in Mathematics*. Springer, 3rd edition, 1999.
- [44] M. Nielsen and I. Chuang. *Quantum Computation and Quantum Information: 10th Anniversary Edition*. Cambridge University Press, 2010.
- [45] R. D’Oliveira, S. El Rouayheb, D. Heinlein, and D. Karpuk. Degree tables for secure distributed matrix multiplication. *IEEE Jour. Sel. Areas in Info. Theory*, 2(3):907918, August 2021.
- [46] L. Hu, M. Nomeir, A. Aytakin, Y. Shi, S. Ulukus, and S. Guha. Entanglement-assisted coding for arbitrary linear computations over a quantum MAC. In *IEEE ITW*, September 2025.